


東海大學生命科學系博士論文

青光眼的分子遺傳學及治療學研究

**Molecular Genetic and Therapeutic Study of  
Glaucoma**



博士班學生：林慧茹

指導老師：范聖興 博士

共同指導老師：蔡輔仁 博士

中華民國 96 年 6 月

<b>Contents</b>	
<b>Acknowledgement</b>	3
<b>Abstract in English</b>	4
<b>Abstract in Chinese</b>	5
<b>Introduction</b>	6
I. Genetic polymorphisms of glaucoma	6
II. Establishing in vitro glaucoma model	12
III. Polyphenols were good candidates to decrease apoptosis of NMDA-treated RGCs	16
IV. The apoptosis pathway of NMDA-treated RGCs	18
<b>Materials and Methods</b>	20
I. Genetic polymorphisms of glaucoma	20
II. Establishing in vitro glaucoma model	23
III. Preparation of polyphenols metabolites	28
IV. Detecting the molecules involved in the apoptosis pathway	30
V. Determining the proteins involved in the polyphenols metabolites and NMDA-treated RGCs by LC-MS-MS	31
VI. <i>In vivo</i> studies of the effects of polyphenol metabolites on NMDA-induced apoptosis of retina ganglion cells	35
VII. Statistical analysis	36
<b>Results</b>	37
I. Genetic polymorphisms of glaucoma	37
II. <i>In vitro</i> model of glaucoma	39
III. The effects of polyphenols metabolites on NMDA-induced apoptosis of N18 RGCs	40
IV. Detecting the apoptosis pathway of aloe-emodin metabolites and NMDA-treated N18 RGCs	42
V. Aloe-emodin metabolites was also effective in decreasing NMDA-induced apoptosis on N18 RGCs <i>in vivo</i>	44
VI. Aloe-emodin metabolites decreased NMDA-induced apoptosis of RGCs by increasing of Cu-Zn superoxide dismutase	44
<b>Discussion</b>	49
I. Genetic polymorphisms of glaucoma	49
II. Aloe-emodin metabolites was effective in decreasing apoptosis of NMDA-induced N18 RGCs	53
III. Aloe-emodin metabolites regulated NMDA-treated N18 RGCs	

by intrinsic apoptosis pathway	54
IV. Aloe-emodin was effective in decreasing apoptosis of N18 RGCs <i>in vivo</i>	54
V. Aloe-emodin metabolites decreased apoptosis of NMDA-treated RGCs by Cu-Zn SOD	55
<b>Conclusion</b>	60
<b>References</b>	61
<b>Figures and legends</b>	80
<b>Tables</b>	112
<b>Curriculum vitae</b>	128

## 誌謝

經過這些年，我明瞭了，讀博士班最大的收穫，不是幫自己多戴一個光環，而是讓自己能有更寬廣及謙卑的心，去面對醫療、研究工作，甚至人生。這些年，在生活中經歷了許多事，幾次想放棄學業，更換工作跑道，但多虧有許多“貴人”讓我選擇了這條既充實又有意義的路。首先感謝東海大學范聖興教授的教導及諸多容忍。謝謝中國醫藥大學蔡輔仁教授的指導，蔡教授的教導常讓我對許多事能豁然開朗，蔡教授洞燭先知，對我而言，不只是研究上的導師，也是做人處事上的良師。也謝謝中國醫藥大學李珮端教授不厭其煩的教導及修改論文，讓我看到了一個學者高尚的典範。但是就在論文完成的前夕李教授病了；這讓許多受過李教授教導的學生都十分不捨，也更讓我們感念到李教授對大家的恩情，祝禱李教授早日康復。此外也謝謝中國醫藥大學陳汶吉教授不斷的鼓勵及諄諄教導；陳汶吉教授博學多聞，與陳教授相處中，常得到許多寶貴的知識及對生命價值的驚喜，陳教授是我的良師益友。感恩東海大學謝明麗教授提供了許多寶貴的意見，從謝教授的建議，可感受到謝教授知識淵博，而自己仍有許多需要學習的地方。也謝謝東海大學劉蕙雯教授及成大曾淑芬教授給我許多建議，讓整個論文更加完整。感謝台大蔡詩偉教授在統計上的教導及幫忙。此外要感謝東海實驗室裡的夥伴：成瀚、小好、青坡、淑芬，大家都視我如家人，這也是我對東海認同的開始。同時也謝謝中國醫藥大學實驗室的阿雅、煒皓、宣嬭、賴建成博士、萬磊博士，及林瑋德學長的幫忙。更要感謝父母給我最大的精神支持，也謝謝老公的包容及鼓勵。還有謝謝二位寶貝孩子，媽咪陪你們讀書，你們也陪媽咪讀書。除此，也需感謝那些讓我有挫折感的人，因為有了挫折感，讓我學會如何更堅強。作為一個醫師、老師、學生、為人子、人妻、人母，我也許都不是最稱職的，但是我會一直努力的。剛進東海，總覺得自己只是過客，但這幾年下來已深深覺得自己是這裡的一份子，此後也將以東海生科為榮。現在結束了在東海的課程，是另一個人生旅程的開始，希望以後也能以從容及積極的態度面對不同的事物。

## Abstract

Glaucoma is a vision-threatening disease and it is the second leading cause of blindness even in a developed area. Since there was no useful predicting methods, some patients appreciate the disease till visual field is constricted. There are many advanced drugs produced recently for controlling intraocular pressure. Nevertheless, there are still some glaucoma patients inevitably lose their vision. In this study, we used single nucleotide polymorphisms (SNPs) to find useful genetic markers for glaucoma in Taiwan. We had found many meaningful SNPs for glaucoma. One of the SNPs which had significant differences was E-cadherin-1 gene 3'-UTR C/T polymorphism. We had found that the incidence of "C" allele of E-cadherin-1 gene 3'-UTR C/T polymorphism was higher in primary open angle glaucoma (POAG) patients. We also established an *in vitro* model of glaucoma by adding NMDA to N18 retina ganglion cells (RGCs). We found that aloe-emodin metabolites were useful in decreasing apoptosis of NMDA-treated N18 RGCs. Aloe-emodin metabolites decreased apoptosis of NMDA-treated N18 RGCs and it was through the intrinsic apoptosis pathway. We also found that the aloe-emodin metabolites were more useful than their parents' form. Moreover, by proteomics study, we detected that Cu-Zn SOD was important in protecting N18 RGCs from NMDA-induced apoptosis. In our study, we excavated useful markers for predicting POAG in Taiwanese and discovered aloe-emodin metabolites were effective in protecting N18 RGCs in an *in vitro* model of glaucoma.

**Key words:** glaucoma, E-cadherin, genetic polymorphism, NMDA, aloe-emodin, Cu-Zn SOD

## 摘 要

青光眼是一種會嚴重危害視力的眼疾，甚至在開發地區青光眼仍是造成失明的第二位，因為沒有有效的預測因子，許多人在視野已經縮小了，才警覺到罹患青光眼。近年來研究開發許多先進的藥物用以控制眼壓。然而，仍有許多青光眼病人最後仍然失明。本研究，我們先以基因多型性來尋找台灣人青光眼的基因標的，我們發現許多對青光眼有意義的基因多型性。其中之一是 E-cadherin 基因的 3'UTR C/T 基因多型性，在開放性青光眼與正常人的差異有顯著的意義。3'UTR C/T 基因多型性中“C”基因型在開放性青光眼的病人中有明顯的增加。此外，我們以 NMDA 加到 N18 視神經細胞，來製造青光眼的體外模式，再以此模式在我們發現蘆薈大黃素的代謝物，能有效的經由內凋零路徑將神經細胞凋零現象減少，我們也發現蘆薈大黃素的代謝產物比它的原始型態更有療效。藉由西方點墨法及螢光報導基因。我們也以蛋白質體學的方式來研究參與此反應的蛋白質，從中發現了 Cu-Zn SOD 對 N18 視網膜神經細胞在受到 NMDA 作用時有保護作用。本研究發現了許多有效的基因標的，用以預知青光眼罹患的可能；並發現在青光眼的體外模式中，蘆薈大黃素可以減少 N18 視網膜神經細胞的凋零現象。

**關鍵詞：**青光眼， E-cadherin， 基因多型性， NMDA， 蘆薈大黃素， 銅鋅超氧化物歧化酶

## **Introduction**

Glaucoma is the second leading cause of blindness in the world, affecting over 70 million people (1). Symptoms of glaucoma include increased intraocular pressure (IOP), cupping and atrophy of the optic nerve head, and finally visual field loss (2). IOP is determined by three factors: the rate of aqueous humor production by the ciliary body, the resistance to aqueous outflow across the trabecular meshwork— Schlemm's canal system, and the level of episcleral venous pressure. Increase of IOP is usually caused by increasing resistance to aqueous humor outflow (3). Nevertheless, glaucoma is a complex disease. Both mechanical and vascular hypotheses have been proposed as the mechanism. The most common form is primary open angle glaucoma (POAG) (4-7). The POAG by definition is not associated with known ocular or systemic disorders which cause the increased resistance to aqueous outflow. POAG patients are virtually asymptomatic, there are at least three definitive signs: elevated intraocular pressure (approximately 21 mmHg or more), enlargement of the optic cup and repeatable field loss (4-7). The POAG usually affects both eyes and may be inherited (8).

### **I . Genetic polymorphisms in glaucoma patients**

Increasing IOP is an important criterion of POAG. Nevertheless, there are many people with IOP above the statistically normal range, who suffer no clinic damage in their life times (ocular hypertension syndrome). In a minority of cases, IOP in the "normal" range is too high for proper functioning of the optic nerve axons (i.e., low-tension glaucoma) (9). Hence IOP level is not used in the definition

of glaucoma. IOP is simply a risk factor for glaucoma and is not the only mechanism causing ganglion cell loss in glaucoma. Rather, elevated IOP damages ganglion cells that have a genetics susceptibility to this stress (10). Those with a first degree relative with glaucoma have up to four times the risk of developing the disease. Due to the lack of predictive markers for glaucoma let many glaucoma patients note the disease only when visual acuity and the visual field have irreversibly deteriorated. The understanding of the genetic background of glaucoma is an important factor for the designing of new treatment for glaucoma. Genetic factors have long been proposed to play an important role in the disease (11, 12). Glaucoma and genetic polymorphisms are not traditionally perceived as being causally related but their relationships were highly suspected and investigated recently (13). In our previous study, we had studied the gene polymorphisms about apoptosis, immunity, tissue morphogenesis and superoxidative stress with POAG (14, 15, 16, 17). In the first part of this report, I presented two results of the studies about genetic polymorphisms and POAG.

### **(1) Association of E-Cadherin gene 3'-UTR C/T polymorphism with POAG**

The most proposed genes responsible for POAG are *myocilin* (*MYOC*) (chromosome position 1q23-q24) and *optineurin* (chromosome position 10p13) genes. Nevertheless, the pathophysiology of POAG is not precisely known and POAG is a multifactorial disease (18, 19). It is not reasonable the assumption that a single gene involved in POAG. POAG may be the result of multiple and interactive genetic and environmental effects. There is a lack of information regarding the genetics of the disease and, hence, the molecular biology of glaucoma is currently under close investigation. In our laboratory, we investigated the relationships of



many genetic polymorphisms among apoptosis, immune and cell morphogenesis. We had already found some single nucleotide polymorphisms (SNPs) associated with POAG (20, 21) and tried to map POAG with genetic polymorphisms.

E-cadherin (E-CDH) is closely related to matrix metalloproteinases (MMP) family which involves in the outflow of aqueous humour in trabecular meshwork. Recently, MMP also attract great attention for the treatments and prostaglandin analogs eye drugs response in POAG (22). Prostaglandin analogs eye drops are believed to lower IOP by increasing the uveoscleral outflow of aqueous humor (23). The effects of these drugs have been proven by eliciting prostaglandin F<sub>2</sub> alpha (FP) receptor, and produce the maximum level of MMP enzymes, thus clearing out the extracellular matrix. The reduction of collagens within the uveoscleral outflow pathway reduces hydraulic resistance and facilitates outflow (24). The disorganization of E-cadherin complexes and the expression of matrix metalloproteinases (MMPs) are frequently involved in the capacity of tissues. MMP/E-cadherin ratio is a significant independent prognostic factor of many diseases (25). Therefore we chose E-CDH as a candidate gene.

Morphogenesis is the process by which cells become organized into distinctive structures and histological patterns in the tissues and organs of the body. In seeking to understand the cellular basis of many diseases, it has been postulated that aberrant morphogenetic processes play fundamental roles in the etiology of many diseases. Cell adhesion is a fundamental determinant of tissue morphogenesis (26-29). CDHs play important roles in tissue morphogenesis, and CDHs comprise a large family of Ca<sup>+2</sup>-dependent, homophilic cell-cell adhesion molecules essential for morphogenic movements and tissue formation during development and for maintenance of tissue integrity in the adult organism (30-32). The CDH family comprises of a large superfamily of cell-surface glycoproteins which have in

common a repeated 110-amino-acid subdomain (call the "cadherin" domain) in their extracellular region (33). CDH-based adhesion is responsible for physiological regulation of CDHs by aberrant function of the signaling pathways. E-CDH is found in many tissues and is among the best understood of the CDHs. E-CDH fragments include the extracellular and transmembrane domains. The shedding the E-CDH extracellular domains which are mediated by metalloproteinases, eliminates the residual adhesive activity and results in a complete disruption of CDH-mediated cell-cell adhesion. Metalloproteinase is a well-known enzyme in the human trabecular meshwork, and is closely involved in the pathogenesis of glaucoma (34-37). The extracellular matrix of trabecular meshwork and lamina cribrosa in the optic nerve are in a constant state of turnover, and several studies have suggested that this homeostasis is out of balance in patients with open angle glaucoma. An increase in collagen synthesis and a decrease in collagen degradation may contribute to the excessive deposit of collagen with loss of the function of trabecular cells during the development of POAG. Recent evidence suggests that matrix metalloproteinases (MMP), which are the enzymes primarily responsible for degradation, play a role in many modern glaucoma therapeutic drugs (35, 36). Direct and indirect regulations of this system increase aqueous humor outflow facility. In addition to the functions of MMP in the trabecular meshwork, MMP can activate microglia and phagocyte which cause the production of cytokines and enzymes that can alter the extracellular matrix in glaucomatous optic nerve heads' lamina cribrosa (37). On the other hand, glaucoma is a complex disease, which involve mechanical or vascular mechanisms. Regardless of the mechanism, the ganglion cells ultimately die by apoptosis, a process which involves the cleavage of E-CDH. The other function of E-CDH is the extruding of apoptotic cells from cell layers (27) and this may relate to the glaucomatous optic neuropathy. That is, the

glaucomatous optic neuropathy may indirectly relate to E-CDH in the basis of apoptosis. Thus, we suspected a relationship between E-CDH and POAG. The human E-CDH gene has been mapped to the long arm of chromosome 16q22.1 which is a site with many stories about genetic events (38, 39). E-CDH mutations in particular diseases may reflect not only the probability of acquiring an E-CDH mutation, but also the extent to which subsequent events preferentially affect the remaining wild-type allele (26). The C/T polymorphism on the CDH-1 gene 3'-un-translated region (UTR) is one of the most important polymorphisms noted. Due to its relatively high frequency, it may be helpful for further genetic studies (40). The C/T polymorphism is at sequence nucleotides (nt) 2797 of E-CDH cDNA, located 54 nt downstream from the TAG stop codon. The E-CDH cDNA sequence can be found in the EMBL/GeneBank database libraries (accession number *Z13009*). The attractive relationship between E-CDH and POAG was worthy to be investigated and we tried to analysis this aspect in molecular field.

## **(2) The distribution of oxidation enzyme eNOS and myeloperoxidase in POAG**

Nitric oxide (NO) is an active biological agent involved in the regulation of diverse physiological and pathological processes. It is synthesized from the amino acid L-arginine by NO synthase. Nitric oxide synthase (NOS) exists as three different isoenzymes: endothelial (eNOS), neuronal (nNOS) and inducible NOS (iNOS) (41). eNOS and nNOS express constitutively and release small amounts of NO. iNOS produces large amounts of NO in response to activation of cells, e.g. by cytokines. To mediate neuro-transmission (42) and vasodilation (43) are two major functions of NO. In the eye, NO regulates the baseline ocular blood flow rate in

response to physiological stress (44) and suppression of NO production reduced the choroidal blood flow (45). A number of studies have indirectly shown that ocular NOS activity may have been increased under physiological stress, e.g. ischaemia (46, 47) and IOP elevation (48, 49). Nevertheless, NO has an unpaired electron, has diverse effects on living cells (50) its inherent free radical nature may impose excitotoxic/oxidative damage on the eye (51). When NO combines with a super-oxide anion ( $O_2^-$ ), they will form a potent and a long-lived oxidant peroxynitrite anion ( $ONOO^-$ ).  $ONOO^-$  may break down into hydroxyl free radical (OH) causing oxidative damage (52) and the generation of more free radicals in a vicious cycle (53). The chain reaction of free radical propagation may account for the time-dependent nature of many diseases (54). Since the total NO level in the retina was consistently higher than that of combined eyecup tissues in both control and IOP-elevated eyes, the retina may be subjected to a significant risk of oxidative damage (55). In present study, we chose eNOS as the candidate for the free radicals study in POAG. Two major gene polymorphisms in eNOS were eNOS intro-4 a-deletion/b-insertion and promoter-786 T to C polymorphism which were already known that associated with many other diseases (56).

Besides,  $NO^\bullet$  can also autoxidize to nitrite ( $NO_2^-$ ) and nitrate ( $NO_3^-$ ) (57).  $NO_2^-$  is a substrate for myeloperoxidase (MPO), a heme enzyme secreted by activated phagocytes, it might also be used for tyrosine nitration in vivo (58). MPO is an abundant enzyme involved in the production of free radicals. Indeed, MPO uses hydrogen peroxide ( $H_2O_2$ ) and  $NO_2^-$  to generate reactive nitrogen species that nitrate tyrosyl residues in vitro (59-61). These reactions might be physiologically relevant because human neutrophils can use the myeloperoxidase- $H_2O_2$ - $NO_2^-$  system to chlorinate and nitrate tyrosine analogues (62). Recently, an important functional single nucleotide polymorphism (SNP) has been identified in the

promoter region of the MPO -463 gene polymorphism, consisting of a G to A substitution. Previous studies have demonstrated that the G allele (in contrast to A allele) creates a strong SP1 binding site, which is correlated with a 25-fold transcriptional enhancement of the gene (63). Despite intense interest in the role of reactive nitrogen species in host defense mechanisms and oxidative tissue injury but there still limited understanding between its relation and POAG. In the present study, we compared the distributions of two major eNOS gene polymorphisms: eNOS intron-4, eNOS promotor-786 and MPO -463 G to A gene polymorphism in POAG patients and normal control.

## **II . Establishing *in vitro* glaucoma model**

### **(1) The current aspect of glaucoma**

The current aspect of glaucoma is that IOP is simple a risk factor for glaucoma but not the only mechanism causing ganglion cell loss in glaucoma. In glaucomatous optic neuropathy, the optic nerve dies by a form of cell death known as apoptosis. Apoptosis is a genetically controlled form of cell death which is controlled by specific genes and their products activated by the dying cell. Many efforts have been proposed to resole the optic nerve death and design the treatment for POAG, but there is still no definite conclusion for POAG. Although the molecular mechanism triggering the apoptosis has not been identified, deprivation of neurotrophic factors (64), ischemia (65), chronic elevation of glutamate (66), and disorganized nitric oxide (NO) metabolism (67) had been suspected to be possible mechanisms. In addition, it was recently suggested that autoantibodies directed toward retinal antigens, such as rhodopsin (68), 60-kDa heat shock protein (hsp 60) (69), 27-kDa heat shock protein (hsp 27), and  $\alpha$ -crystallin (1) may be involved in facilitating apoptotic cell death in some glaucoma patients, particularly in NTG.

However, it has become clear that it may be helpful to look beyond pressure control in the treatment of glaucoma. This premise underlies the concept of direct neuroprotection in glaucoma, whereby agents are sought that may retard glaucomatous loss without necessarily affecting the IOP.

## **(2) The functions of N-methy-D-aspartate (NMDA) in glaucomatous eyes**

The ability of the nervous system to rapidly convey sensory information and complex motor commands from one part of the body to another and to form thoughts and memory is largely dependent on a single powerful excitatory neurotransmitter, glutamate. There are other excitatory neurotransmitters in the brain, but glutamate is the most common and widely distributed. Most neurons contain high concentrations of glutamate (10 mM) which is used in tightly controlled quantities and for very brief amounts of time (milliseconds) to communicate with other neurons via synaptic endings (70). Because glutamate is so powerful, however, its presence in excessive amounts or for excessive periods of time can literally excite cells to death (71). These phenomena are later coined to the term “excitotoxicity” (72, 73). A variety of naturally occurring conditions can lead to the excessive release of glutamate within the nervous system and, thus, lead to cell death. When the nervous system suffers a stress insult, large amounts of glutamate are released from injured cells. These high levels of glutamate wash over thousands of nearby cells that had survived the original trauma, causing them to depolarize, swell, lyse, and die. The lysing cells release more glutamate leading to a cascade of autodestructive events and progressive cell death that can continue for hours after the original injury (72, 73). A similar phenomenon occurs in stroke; the ischemic event deprives many neurons of the energy they need to maintain ionic

homeostasis, causing them to depolarize, lyse and die (70, 74). A slower subtle form of excitotoxicity is implicated in a variety of slowly progressing neurodegenerative disorders. In disorders, such as Huntington's disease, Parkinson's disease, Alzheimer's disease, multiple sclerosis and glaucoma suffer moderately elevated glutamate concentrations for longer periods of time (than occur during normal neurotransmission) trigger cellular processes in neurons that eventually lead to apoptotic-like cell death. This type of slow, apoptotic-like excitotoxicity is also implicated in glaucoma (75-80). Under normal conditions of synaptic transmission, the NMDA-receptor channel is activated for brief periods of time only. When NMDA receptor is activated, it opens a channel that allows  $\text{Ca}^{+2}$  to move into the cell. In some areas of the brain, this activity is important for long-term potentiation a cellular/electrophysiological correlate of learning and memory formation (76-79). Under pathological conditions, however, chronic low-grade overactivation of the receptor causes an excessive amount of  $\text{Ca}^{+2}$  influx into the nerve cell which then triggers a variety of processes that can lead to apoptosis. These include  $\text{Ca}^{+2}$  overload of mitochondria, resulting in oxygen free radical formation and activation of caspases;  $\text{Ca}^{+2}$  dependent activation of neuronal nitric oxide synthase (NOS), leading to increased nitric oxide (NO) production and the formation of toxic peroxynitrite ( $\text{ONOO}^-$ ); and stimulation of mitogen-activated protein kinase p38 (MAPK p38), which activates transcription factors that can enter the nucleus, influence neuronal injury and induce apoptosis (80-89). Although there are several classes of glutamate receptors, excitotoxic retinal ganglion cell loss primarily results from glutamate binding to the NMDA subtype (78, 79). Additionally, excitotoxic mechanisms can play even with normal levels of glutamate if NMDA receptor activity is increased, for example, when retinal ganglion cell neurons are injured and thus become depolarized; this condition relieves the normal block of the

ion channel by  $Mg^{2+}$  and thus abnormally increases NMDA receptor activity (80-90). Excitotoxicity is a particularly attractive target for neuroprotective efforts because it is implicated in the pathophysiology of a wide variety of acute and chronic neurodegenerative disorders (90). Recent experimental findings are consistent with the notion that glutamatergic excitotoxicity may be a contributing factor in glaucomatous injury to retinal ganglion cells (RGCs). The concentration of vitreal glutamate has been shown to be elevated in humans (91) and dogs (92) with primary glaucoma, as well as in monkeys (91) with experimentally induced glaucoma. When, with use of intravitreal dosing, the vitreal glutamate concentration in rats was maintained at the same levels observed in glaucoma subjects, significant RGC loss was observed. The increase in IOP associated with glaucoma may lead directly to a secondary increase in vitreal glutamate, or there might be other pathologic steps involved (93). However, if the glutamate level in the rat eye chronically raised to the concentration as in human eyes with glaucoma, 50% of the retinal ganglion cells die 3 months later. Therefore, even if glutamate elevation is only an epiphenomenon associated with glaucoma, it may contribute to ganglion cell loss in humans. If interventions can be identified that retard the toxic effects of glutamate, glaucomatous visual slowly loss. These findings indicate that glutamate elevations and excitotoxicity, no matter they are etiologies or results, may play important roles in the optic nerve pathology in the glaucomatous eyes (50). There were some *in vitro* glaucoma models, include adding antibody of Hsp 27 to RGCs, depriving  $O_2$  in RGCs to induce ischemia, changing pressure of RGCs. Among the mechanisms of glaucoma, NMDA induced apoptosis of RGCs is a well-accepted etiology and it is the most common used model of glaucoma. In this study, we used NMDA-induced apoptosis of N18 RGCs to mimic glaucoma optic neuropathy *in vitro*. Using the glaucoma model we screened the flavonoids from Chinese herbs to



decrease the apoptosis of RGCs induced by NMDA. Besides, we also used injection of NMDA to the mouse's eyes to induce RGCs' apoptosis in order to mimic glaucomatous optic neuropathy *in vivo*.

### **III. Polyphenols were good candidates to decrease apoptosis of NMDA-treated RGCs**

In 1930 a new substance was isolated from oranges, which is believed to be a member of a new class of vitamins, and was designated as vitamin P and at least known as polyphenols (95, 96). Polyphenols belong to a group of natural substances with variable phenolic structures and are found in fruit, vegetables, grains, bark, roots, stems, flowers, tea, and wine (97). These natural products were known for their beneficial effects on health long before polyphenols were isolated as the effective compounds. More than 4000 varieties of polyphenols have been identified, many of which are responsible for the attractive colors of flowers, fruit, and leaves. Information on the working mechanisms of polyphenols was scarce in the past. However, it has been widely known for centuries that derivatives of plant origin possess a broad spectrum of biological activity (98). Research on polyphenols received an added impulse with the discovery of the French paradox, i.e., the low cardiovascular mortality rate observed in Mediterranean populations in association with red wine consumption and a high saturated fat intake (99, 100). The polyphenols in red wine are responsible, at least in part, for this effect. Furthermore, epidemiologic studies suggest a protective role of dietary polyphenols against coronary heart disease. The association between polyphenols intake and the long time effects on mortality was studied subsequently and it was suggested that polyphenols intake was inversely correlated with mortality due to anti-allergic (101),

antiviral (102), anticancer (103), and antioxidation properties (104). Polyphenols can be divided into various classes on the basis of their molecular structure. The most important effect of flavonoids is the scavenging of oxygen-derived free radicals. Body cells and tissues are continuously threatened by the damage caused by free radicals and reactive oxygen species. Reactive oxygen species are produced during normal oxygen metabolism or are induced by events which free radicals interfere with cellular functions and results in cellular membrane damage. This cellular damage causes a shift in the net charge of the cell, changing the osmotic pressure, leading to swelling and eventually cell death. Free radicals can attract various inflammatory mediators, contributing to a general inflammatory response and tissue damage. Polyphenols may have an additive effect to the endogenous scavenging compounds. Polyphenols can interfere with free radical-producing system, they can also increase the function of the endogenous antioxidants (105, 106).

Polyphenols are primarily present as glycosides in nature. There are studies indicating that polyphenol aglycosides are not absorbed per se and the major molecules circulating in blood are polyphenol aglycones glucuronides/sulfates; whereas only a small amount of polyphenol glycosides are present in the circulation. The absorption of polyphenol glucoside's parent forms are speculated that they are transported across gut by the intestinal sodium-glucose transporter. Upon hydrolysis by the enzymes released by enterobacteria, the sugar moiety of polyphenol glycosides were cleaved and resulted in more lipophilic aglycones, which become permeable through the gut wall. This can be explained as the attached sugar moiety on the polyphenol affected the rate of hydrolysis of glycosides and the absorption of their aglycones (107). Aglycone form polyphenol are absorbed more rapidly to

result in much earlier  $T_{\max}$  and higher  $C_{\max}$  of its conjugated metabolites and eliminated faster (108). There is very large amount of *in vitro* data of polyphenols, but very few available reports of animal studies. Furthermore, information concerning the biologic fates of polyphenols is very limited. In this study, we use polyphenol conjugated forms as the theme to detect the effects of polyphenols conjugated forms in the apoptosis retinal ganglion cells. The polyphenol conjugated forms used in this study are obtained from the digestive products after giving rabbits with polyphenol nature type (109, 110). Polyphenols are valid antioxidants, polyphenol conjugated forms are their major compounds work in the body. In this study, we investigate the effects of polyphenol conjugated forms on NMDA induced glaucomatous neuropathy both *in vitro* and *in vivo*, the signaling pathway which the polyphenol conjugated forms are by way of and the proteins involve in the reactions. Polyphenol used in this study included: morin [extracted from *Morus alba* (桑白皮)] (111), naringenin [extracted from *Citrus sinensis Osbeck* (枳實)] (112), hesperetin [extracted from *Citrus reticulata Blamco* (陳皮)] (113), radix puerariae [extracted from *pueraria lobata Ohwi* (葛根)] (114), emodin [extracted from *Rheum palmatum* (大黃)] (115) and aloe-emodin [extracted from *Rheum palmatum* (大黃)] (116). In this study we compared the metabolites form of the Chinese herbs and some well-known neuroprotectors in protecting NMDA-induced apoptosis of RGCs.

#### **IV. The apoptosis pathway of NMDA-treated RGCs**

We detected apoptosis pathway of the polyphenols and NMDA-treated RGCs. In general, apoptosis is activated by two main pathways: the receptor-mediated pathway and the intrinsic (mitochondrial) pathway. Components of the FAS/FAS

ligand system represent the prototypical receptor-mediated apoptosis pathway. Intrinsic pathway does not involve a surface receptor, but rather is formed by the modification of intracellular pools of proteins. Environmental or intracellular stressors result in post-translation modification of proteins in intrinsic pathway, which then exert their effect on the mitochondria to release cytochrome c. The released cytochrome c then binds with apoptosis-activating factor-1 and caspase-9 to form a complex known as the apoptosome, which in turn activates more downstream apoptotic reactions. Understanding the apoptosis pathway of the reaction helped us in realizing the mechanism of the disease and the effects of the polyphenols.

## **Materials and Methods**

### **I . Single nucleotide polymorphisms of glaucoma patients**

From May 2000 to July 2000 we enrolled POAG patients from the department of Ophthalmology at the China Medical University Hospital. All patients in this study received serial ophthalmic examinations which included IOP, visual acuity, automated perimetry, gonioscopy, optic disc examination and retinal examinations. The volunteers in the control group were selected from the patients who received routine physical examination and were examined by the same ophthalmologist. Volunteers were all free of any systemic diseases including cardiovascular, reproductive and urologic diseases. Volunteers suspected of having glaucoma were excluded from the study. Patients with ocular diseases other than POAG were also excluded from our study. All patients included in this study had POAG patients and met at least one criterion from each of the following categories.

Visual field criteria:

- 1) At least two abnormal visual field tests by Humphrey automated perimetry, as defined by computer-based objective criteria.
- 2) The presence of one or more absolute defects in the central visual field 30°, with ophthalmologic interpretation as glaucomatous visual field loss.

Optic disc criteria: (optic disc damage present in fundus photographs)

- 1) Either a horizontal or vertical cup-to-disc ratio of 0.6 or more.
- 2) Narrowest remaining neuroretinal rim was 20% or fewer disc diameters.

Ophthalmologic criteria:

Patients with other possible causes of disc and field changes other than POAG were

excluded.

We investigated the CDH-1 gene 3'-UTR in all subjects. The prevalence of the polymorphism was compared between the control group and patient group. Odds ratio was used to calculate the frequencies of the different alleles. This study was carried out with approval from the Human Study Committee of the China Medical University Hospital. Informed consent was obtained from all patients who participated in this study. The POAG group consisted of 60 patients and the control group was made up of 103 healthy volunteers in this study. The volunteers ranged in age from 52 to 71 years old (mean: 50 years), and were free from any ophthalmic diseases. The volunteers were all Chinese and unrelated. There were 51 females and 52 males. The POAG patients ranged in age from 20 to 70 years old (mean: 55 years) and were unrelated. There were 30 females and 30 males.

The genomic DNA was prepared from peripheral blood by a DNA Extractor WB kit (Wako, Japan). Polymerase chain reactions (PCRs) were carried out to a total volume of 50  $\mu$ l, containing genomic DNA, 2-6  $\mu$ mole of each primer, 1X Taq polymerase buffer (1.5 mM MgCl<sub>2</sub>), and 0.25 units of AmpliTaq DNA polymerase (Perkin Elmer, Foster City, USA). The primer for the E-CDH gene 3'-UTR polymorphism was designed by amplifying the created restriction site (ACRS): forward (5'-CAGACAAAGAC CAGGACTAT-3') and reverse (5'-AAGGGAGCTGAAAAACCACCAGCCAC-3'). PCR amplification was performed in a programmable thermal cycler GeneAmp PCR System 2400 (Perkin Elmer). The cycling condition for CDH-1 was set as follows: one cycle at 94°C for 5 min, 35 cycles at 94°C for 30 sec, 56°C for 30 sec, and 72°C for 30 sec, and, one final cycle of extension at 72°C for 7 min. The PCR product of 172-bp was mixed with 2 units *Pml* I (New England Biolabs, Beverly, USA) and the reaction

buffer according to the manufacturer's instructions. For future reference, two fragments of 146-bp and 26-bp will be present if the product is digestable (Fig. 1). The reaction buffer and PCR product was incubated at 37°C for 3 hours. Then, 10 µl of the product was loaded onto 3% agarose gel containing ethidium bromide for electrophoresis. The resulting products were classified as digestable (CC homozygote), undigestable (TT homozygote) and combined C/T heterozygote. Statistical analysis of the frequency of allele distribution in this polymorphism in the control and POAG patient groups was compared by the chi-square test. The software used for the calculation was the SPSS® system with sample power analysis. Results were considered statistically significant when the probability of findings occurring by chance was less than 5 % (p<0.05). Odds ratios (OR) with 95 % confidence intervals were calculated in order to estimate the risk of suffering POAG between genotypes.

PCR was used to identify the genotypes of all of the NO and MPO related genes. PCR of the polymorphisms was carried out to a total volume of 50 µl, containing genomic DNA (2-6 pmole of each primer); 1X Taq polymerase buffer (1.5 mM MgCl<sub>2</sub>); and 0.25 units of AmpliTaq DNA polymerase (Perkin Elmer, Foster City, USA). The primers used for the PCR reaction were 5'-CGGTATAGGCACACAATGGTGAG-3' (forward primer) and 5'-GCAATGGTT CAAGCGATTCTT-3' (reverse primer).

For the eNOS intron -4, 10 µl of the products were loaded into 3% agarose gel containing ethidium bromide for electrophoresis and each allele was recognized according to its size. The eNOS polymorphism at intron-4 was analyzed by PCR amplification followed by restriction analysis using *NgoMIV* (New England Biolabs, Beverly (USA) digestion. The a-deletion/b-insertion and b-insertion allele showed

up as 190-bp and 114-bp on agarose electrophoresis. The b-insertion allele was 304-bp. The region containing the polymorphic site within promoter -786 of the eNOS gene was amplified and then digested by *Taq* I (New England Biolabs). The T allele was 135 bp+114 bp and The C allele was 249-bp as shown on electrophoresis. The molecular analyses of patients and controls are performed in the same laboratory at the same time and that the gels are inspected by investigators who are masked to the clinical phenotype of the individuals being studied. The MPO polymorphism at position -463 was analyzed by PCR amplification followed by restriction analysis using *Ava* I (New England Biolabs, Beverly (USA) digestion. The primers used for the PCR reaction were 5'-CGGTATAGGCACACAATGGTGAG-3' (forward primer) and 5'-GCAATGGTT CAAGCGATTCTT-3' (reverse primer).

## **II. Establishing *in vitro* glaucoma model**

### **Retina ganglion cell line (N18)**

N18 RGCs line was obtained from Japanese Collection of Research Bioresources Bank. N18 RGCs was rat retina ganglion cells hybrid with lymphoma cells. The cells were placed into 75 cm<sup>3</sup> tissue culture flasks and grown at 37°C under a humidified 5% CO<sub>2</sub> and 95% air at one atmosphere in Dulbecco's modified Eagle's medium (DMEM) (Merck Co. [ Darmstadt, Germany ] ) supplemented with 10% FBS (Gibco BRL [Grand Island, NY, USA]), 1% penicillin-streptomycin (10 ng/ml penicillin and 10 ng/ml streptomycin) (Gibco BRL [Grand Island, NY, USA]), each of nonessential amino acids, vitamins and 1% glutamine (Gibco BRL [Grand Island, NY, USA]). The cells were at a density of 20 × 10<sup>4</sup> cells/ flask at a final volume of 12 ml or on 6-well plates at a density of 3×10<sup>4</sup> cells/well at a final volume of 2 ml/well. Cells grown to approximate confluence then were incubated in



different condition. HAT (Hypoxanthine – Aminopterin – Thymidine) medium (Sigma Chemical Co. [St. Louis, MO, USA]) was used to select hybridomas among normal cell populations. The cells had been cultured for several generations and checked for viability. To confirm the property of N18 cells, we stained the cells with anti-Thy-1 antibody, a specific marker for granulocytic linkage and neurons. In addition, the cells also checked with anti-NMDA receptor antibody and stained for proving the existence of NMDA receptors. To examine the effects of NMDA with different concentrations, 50 –500  $\mu$ M NMDA were added and cells were incubated for 24 hours before cell viabilities were checked.

### **Flow chart of the experiment**

RGCs grown to approximate confluence then different flavonoid metabolites are added for 24 hours. For opening the channels of NMDA receptors,  $Mg^{2+}$  free HBS buffer was added. For simulating apoptosis of RGCs to mimic glaucomatous neuropathy, cells were exposed to NMDA with different concentrations for 24 hours. After incubation, the cells were washed with PBS solution and detected cells viability by flow cytometry. The experiments cells were separated into four groups: 1. Only NMDA was added, 2. NMDA and flavonoids were added, 3. Only flavonoids were added, 4. Neither NMDA nor flavonoids was added. Moreover, the effects of flavonoids metabolites were also tested in experiments *in vivo*. The flavonoid and NMDA was delivered into mice' eyes by sub-conjunctiva injection. The eyes were enucleated for histological examinations 24 hours after drugs were given.

Flow cytometry used for analysing cell viability, mitochondrial membrane potential and  $\text{Ca}^{2+}$  concentrations.

### **(1) Cells preparation**

For detecting the surface or extracellular antigen, cells were washed twice after treated with different conditions. Re-suspended with the given antibody, and incubated at 4 °C for 35-min staining. After being washed three times with 10% FBS in RPMI 1640 with 0.1% sodium azide, cells were stained with FITC labeled secondary antibody (goat anti-rat IgG; Jackson Immuno Research Laboratories, West Grove, PA) at 4 °C for 35 min. The cells were then washed three times, re-suspended in PBS, and analyzed by flow cytometry. For detecting the intracellular antigen, cells were initially washed twice, re-suspended in 100 ml of ice-cold 1% formaldehyde for 5 min, and mixed with 100 ml of ice-cold 99% methanol for 30 min. Then the cells were washed three times with 0.1% BSA in PBS and mixed with 100 ml of 0.1% Triton X-100 in PBS with 0.1% sodium citrate on ice for 45 min. After being washed three times with the same buffer, the cells were incubated with polyclonal or monoclonal antibody at 4 °C for 35-min staining and then washed three times with 0.1% BSA in PBS. The subsequent procedures were equivalent to those for detection of surface antigen.

### **(2) Using flow cytometry to determine cell viability**

The N18 cells were plated in 12 well plates at a density of  $5 \times 10^5$  cells/well and grown for 24 hours and grown at 37°C, 5% CO<sub>2</sub> and 95% condition. For determining cell viability, the flow cytometric (Becton Dickinson FACS Calibur) assays are used as described previously. Two fluorescent dyes are used to detect the cells viability (117-119). Propidium iodide (PI) (42µM) (Sigma Chemical Co. [St.

Louis, MO, USA]) is a fluorescent dye that binds specifically to DNA. This property had led to its common use in evaluation of cell cycle and apoptosis by flow cytometry. When excited by a laser light at 488 nm, PI emitted a signal that could be monitored by the red wavelength. PI was excluded from viable cells, thus analyzed of DNA content in cells requires membrane permeabilization. In evaluation of apoptosis, PI was used to distinguish necrotic cells or cells in late stages of apoptosis, which had permeabilized membranes and thus bind PI, from viable cells or cells in early apoptosis where membranes were intact and PI was excluded. Thiazole orange (TO) (4.3mM) (Sigma Chemical Co. [St. Louis, MO, USA]) would increase 18,900 times fluorescence quantum upon binding to DNA. All cells containing DNA were stained with the permeant dye (TO), and fluoresced yellow to orange. Simultaneously, cells with damaged membranes were stained with the impermeant dye, propidium iodide (PI), and fluoresce orange to red. Flow cytometry allowed evaluation of disinfectant or preservative efficacy in as short as 30 minutes and allowed the quantitation of live and dead cells (117-119).

### **(3) Using flow cytometry to analyse for mitochondrial membrane potential**

Cells were prepared as above descriptions. For detect mitochondrial membrane potential, retina cells were stained by DiOC<sub>6</sub>. DiOC<sub>6</sub> was a lipophilic fluorescence, it stained mitochondria in living cells and it was a positively charged molecule that permeated through the plasma membrane. The cells were harvested and washed twice, re-suspended in 500 µl of DiOC<sub>6</sub> (4 mol/L) and incubated at 37 °C for 30 min and analyzed by flow cytometry (117). A decreasing of DiOC<sub>6</sub> fluorescence would be caused by the reducing of mitochondrial membrane potential.

#### **(4) Using flow cytometry to detect the Ca<sup>2+</sup> concentrations in N18 RGCs**

The levels of Ca<sup>2+</sup> of the retina ganglion cells were determined by flow cytometry (Becton Dickinson FACS Calibur), using the Indo 1/AM (Calbiochem; La Jolla, CA). The cells treated with different condition were harvested and washed twice and were re-suspended in Indo 1/AM (3  $\mu$ g/ml) and incubated at 37°C for 30 min and analyzed by flow cytometry (120).

#### **RNA isolation**

RNA was extracted from rat retinal cell (N18-RE-105) cells using 250  $\mu$ l TRIZOL reagent according the manufacturer's direction (Biotechx, Friendswood, TX). The protocol includes cell lysis, extraction of the organic phase with chloroform, and precipitation of RNA with isopropanol. RNA concentrations would be calculated from the absorbance at 260 nm. An aliquot containing 0.2  $\mu$ g of total RNA would be mixed with dNTP (20  $\mu$ M), 3'primer (0.25  $\mu$ M), reverse transcription buffer (1x, BRL) in a total volume of 19 $\mu$ L and will be heated at 65 °C for 5 min and at 37 °C for 10 min, 1  $\mu$ L MMLV reverse transcriptase (200  $\mu$ L) would be added and incubated at 37 °C for 50 min, followed by 95 °C for 5 min to inactive the reverse transcriptase. At the end of the transcription, set the tubes on ice for PCR or store at -20 °C later use.

#### **Special retina cells preparation**

##### **(1) Separate cytosolic fraction from others**

After retina ganglion cells were washed twice with HBSS and scraped, on ice, into ice-cold lysis buffer containing 20 mM Tris-HCl, pH 8.0, 0.5 mM EDTA, 0.5 mM EGTA, 25 mgrml leupeptin, 10 mgrml antipain, 10 mgrml pepstatin, 1 mM dithiothreitol, and 2.5 mM phenylmethylsulfonyl fluoride. The cells were collected

and sonicated for 10 pulses. The sonicated samples were centrifuged at 100,000×g for 30 min at 4°C and the resulting supernatant was collected as the “cytosolic” fraction. The pellet was resuspended in lysis buffer plus 0.5% Triton X-100, sonicated, and centrifuged as before. The supernatant was collected as the “particulate” fraction. Protein kinase C activity in both fractions is determined.

## **(2) Preparation of nuclear extract**

Assays were performed as described previously with modification (121). In brief, cells were harvested and washed twice with cold phosphate buffer saline (PBS) buffer. The pellet was resuspended in cytosolic buffer (10 mM HEPES, pH 7.9, 1.5 mM MgCl<sub>2</sub>, 10 mM KCl, 0.5 mM DTT, 0.5 mM phenylmethylsulfonyl fluoride (PMSF), 0.3% Nonidet P-40, 1 mg/ml leupeptin, 1 mg/ml aprotinin) on ice for 15 min and the supernatants were collected as cytoplasmic extracts after centrifugation with 2000×g for 10 min. The pellets were resuspended with nuclear protein extraction buffer (20 mM HEPES, pH 7.9, 0.45 M NaCl, 25% (v/v) glycerol, 1.5 mM MgCl<sub>2</sub>, 0.2 mM EDTA, 0.5 mM DTT, 0.5 mM PMSF, 1 mg/ml leupeptin, 1 mg/ml aprotinin) and incubated on ice for 30 min. The nuclear proteins were collected by centrifugation with 20,000×g at 4°C for 15 min. The activity of c-jun is detected in nuclear extraction.

## **III. Preparation of polyphenols metabolites**

### **(1) Chemicals used in preparation of polyphenols metabolites**

Parents' forms of polyphenols, PEG 400 and acetic acid (99%) were purchased from Sigma Chemical Co. (St. Louis, MO, USA). LC grade acetonitrile, ethyl acetate and methyl alcohol were obtained from Mallinckrodt Baker, Inc.

(Phillipsburg, NJ, USA). L (+)-Ascorbic acid was obtained from RdH Laborchemikalien GmbH & Co. KG (Seelze, Germany). Sodium acetate was purchased from Kohusan Chemical Works, Ltd. (Tokyo, Japan). Milli-Q plus Water (Millipore, Bedford, MA, USA) was used for all preparations.

## **(2) Administrating of polyphenols to rats**

Male Sprague-Dawley rats weighing 250~300 g were fasted for 12 h before drug administration. Parents' form of polyphenols were dissolved in PEG 400 (10 mg/mL) and intravenously administered to rats at a dose of 5 mg/kg. Blood was withdrawn via cardiac puncture at 5 min post dosing and the serum was obtained after centrifugation at 9860 g for 15 min. The animal study adhered to "The Guidebook for the Care and Use of Laboratory Animals (2002)" (Published by The Chinese Society for the Laboratory Animal Science, Taiwan, R.O.C.).

## **(3) Preparation and quantification of polyphenols metabolites in serum**

Serum was vortexed with 4-fold volume of methanol, then centrifuged at 9860 for 15 min to remove the precipitate. The supernatant was evaporated under vacuum. The residue was then dissolved in water and purified through solid phase extraction using Strata (Phenomenex, USA) to remove the parents' forms of flavonoids. The concentrations of glucuronides and sulfates of polyphenols in serum were determined after hydrolysis with  $\beta$ -glucuronidase and sulfatase, respectively. For glucuronide quantitation, 100  $\mu$ L sample was mixed with 50  $\mu$ L  $\beta$ -glucuronidase (1000 units/mL in pH 5 acetate buffer), 50  $\mu$ L ascorbic acid (100 mg/mL) and incubated at 37°C for 4 h under anaerobic condition and protected from light. On the other hand, 100  $\mu$ L sample was mixed with 50  $\mu$ L sulfatase

(1000 units/mL in pH 5 acetate buffer), 50  $\mu$ L ascorbic acid (100 mg/mL) and incubated at 37°C for 2 h under anaerobic condition and protected from light. After enzymatic hydrolysis, serum was partitioned with 200  $\mu$ L ethyl acetate (containing 1  $\mu$ g/mL of emodin as internal standard). The ethyl acetate layer was evaporated under N<sub>2</sub> gas to dryness and reconstituted with an appropriate volume of mobile phase, then 20  $\mu$ L was subjected to HPLC analysis.

#### **(4) HPLC conditions for preparation polyphenols metabolites in serum**

The HPLC apparatus included two pumps (LC-10ATvp, Shimadzu, Japan), an UV spectrophotometric detector (SPD-10Avp, Shimadzu, Japan). The RP-18 column (Cosmosil, 250×4.6 mm) was equipped with a prefilter. The mobile phase was acetonitrile : 0.1% ortho-phosphoric acid (52:48, v/v) and the flow rate was 1.0 mL/min with the detection wavelength set at 250 nm. The nitrogen evaporator (N-Evap<sup>TM</sup> 112) was supplied by Organomation Associates, Inc. (USA).

#### **IV. Detecting the molecules involved in the apoptosis pathway**

We used Western blotting to detect the molecules involved in the apoptosis pathway of NMDA-treated N18 RGCs. After washing the cells with phosphate-buffered saline, they were lysed in sample buffer (1% SDS, 100 mM dithiothreitol (DTT), 60 mM Tris, pH 6.8, 0.001% bromophenol blue). Protein concentrations are determined using the BCA method (Sigma). The samples are boiled for 5 minutes before subjecting them to electrophoresis. Samples (50 mg of total protein) are separated by electrophoresis in 10% to 15% sodium dodecyl sulfate polyacrylamide gels at 160 V for 1 h and electrophoretically transferred to polyvinylidene fluoride membranes (Millipore, Marlboro, MA) using a semi-dry transfer system (BioRad, Hercules, CA). After transfer, membranes was blocked in a

buffer (50 mM Tris-HCl, 154 mM NaCl, 0.1% Tween-20, pH 7.5) containing 5% nonfat dry milk for 1 h and then overnight in the same buffer containing a dilution of primary antibody and sodium azide. Primary antibodies are monoclonal antibodies to the molecules to be detected (antibodies for caspase-3, caspase 9, p53 and bax, respectively) (Pharmingen, San Diego, CA) and were used at a dilution of 1:1000. After several washes and the second blocking for 20 min, the membranes are incubated with a dilution of secondary antibodies conjugated with horseradish peroxidase (Fisher Scientific, Pittsburgh, PA) at 1:2000 for 1 h. Immunoreactive bands were visualized by enhanced chemiluminescence using commercial reagents (Amersham Life Science, Arlington Heights, IL). Densitometric measurements of the bands obtained from Western blot analysis were made using a digitalized scientific software program (Kodak ID 3.5 purchased from Kodak). All data were normalized to the control group.

## **V. Determining the proteins involved in the polyphenols metabolites and NMDA-treated RGCs by LC-MS-MS**

### **(1) Two dimensional gel electrophoresis (2-DE) and image analysis to evaluate proteins expressed in different condition**

An aliquot containing 100 µg of protein sample was diluted with 350 µl of rehydration buffer containing 8M urea, 4% CHAPS, 65mM DTE, 0.5% ampholytes and a trace of bromophenol blue. Sample was hydrated on a 17 cm strip and immobilized to pH gradient pH 3-10 (ReadyStrip IPG strip, Bio-Rad) overnight; sample were focused for a total of 60 kVhr (PROTEAN IEF cell, Bio-Rad) at 20°C and then stored at -80°C. Strips were equilibrated with 3 ml of a equilibrium solution containing 50mM Tris-HCl (pH 8.8), 6M urea, 30% glycerol, 2% SDS, a



trace of bromophenol blue, and DTE (1% w/v) for 20 min, followed by equilibration for 20 min in the same solution containing iodoacetamide (2.5% w/v) instead of DTE. The strips were transferred to the top of 12% polyacrylamide gels and held in position with molten 0.5% agarose in running buffer containing 25mM Tris, 0.192M glycine, 0.1% SDS. Gels were run at 16mA for 30 min followed by 50mA for 4~5 hour. Gels were routinely stained with silver nitrate and then scanned by GS-800 imaging densitometer with PDQuest software version 7.1.1 (Bio-Rad). To evaluate intrasample and inter-sample variability, gels were analyzed in the following manner. Protein spots from each gel were detected and matched automatically. A master gel image was generated from the matched gel sets. Finally, the intensity of the spots was compared among gels. Data were exported to Microsoft Excel for creation of the correction graphs and spot intensity graphs.

## **(2) In-gel protein digestion of proteins from silver stained gels for nano-LC-MS/MS**

A slightly modified procedure originally developed by Terry et al. was used for in-gel digestion of proteins from silver stained gels for nano-LC-MS/MS (122). Briefly, each spot of interest in the silver stained gel was sliced into 1 mm cubes. The proteins in these gels were reduced and methylated with 50 mM Dithioerythritol (DTE) and 100 mM Iodoacetamide (IAA) in 50 mM ammonium bicarbonate. These gel pieces were washed two times with 50% v/v ACN in 100 mM ammonium bicarbonate buffer (pH 8.0) for 10 min at room temperature. They were then soaked in 100% ACN for 5 min, dried in a lyophilizer for 20–30 min and rehydrated in 50 mM ammonium bicarbonate buffer (pH 8.0) containing 10 µg/mL

trypsin (Promega, Madison, WI, USA) until the gel pieces were fully immersed. After incubating for 16–20 h at 30°C, the remaining trypsin solution was transferred into a new microtube. The gel pieces were resuspended with 50% ACN in 5.0% FA for 60 min and then concentrated to dryness.

### **(3) Nanoelectrospray mass spectrometry to analyze the meaningful proteins involved in the reaction**

Nanoscale capillary LC-MS/MS was used to analyze the meaningful proteins involved in the reaction. LC-MS/MS analysis was performed using an Ultimate capillary LC system (LC Packings, Amsterdam, The Netherlands) coupled to a QSTARXL quadrupole-time of flight (Q-TOF) mass spectrometer (Applied Biosystem/MDS Sciex, Foster City, CA, USA). The nanoscale capillary LC separation was performed on a RP C18 column (15 cm×75 μm i.d.) with a flow rate of 200 nL/min and a 60 min linear gradient of 5-50% buffer B. Buffer A contained 0.1% formic acid in 5 % aqueous ACN; buffer B contained 0.1% formic acid in 95% aqueous ACN. The nanoLC tip for on-line LC-MS was a PicoTip (FS360-20-10-D-20; New Objective, Cambridge, MA, USA). Data were acquired by automatic Information Dependent Acquisition (IDA; Applied Biosystem/MDS Sciex). The IDA automatically finds the most intense ions in a TOF MS spectrum, and then performs an optimized MS/MS analysis on the selected ions. The product ion spectra generated by nanoLC-MS/MS were searched against NCBI databases for exact matches using the ProID program (Applied Biosystem/MDS Sciex) and the MASCOT search program (<http://www.matrixscience.com>) (123). A mammalian taxonomy restriction was

used and the mass tolerance of both precursor ion and fragment ions was set to  $\pm 0.3$  Da. Carbamidomethyl cysteine was set as a fixed modification, while serine, threonine, tyrosine phosphorylation and other modifications were set as variable modifications. All phosphopeptides identified were confirmed by manual interpretation of the spectra.

#### **(4) Quantitative polymerase chain reaction (Q-PCR) to investigate the quantity of RNA in the reaction**

Q-PCR was used to investigate the quantity of RNA in the reaction. Total RNA was extracted with TRIZOL reagent (Invitrogen) according to the manufacturer's protocol. For each cDNA sample, a ratio of the relative amounts of target gene and GAPDH was calculated to compensate for variations in quantity or quality of starting mRNA, as well as for differences in reverse transcriptase efficiency. The fold change in the target gene relative to the GAPDH endogenous control gene specific forward and reverse primers were designed using the LightCycler Probe Design software (Roche Applied Science), based on sequence data from the hemerythrin nucleic acid sequence. The primer sequences and reactive conditions were listed in the Table 1. The fold change in the target gene relative to the GAPDH endogenous control gene was calculated according to a method previously proposed (124),  $\text{fold change} = 2^{\Delta(\Delta CT)}$  where  $\Delta CT = CT_{\text{target}} - CT_{\text{GAPDH}}$  and  $\Delta(\Delta CT) = \Delta CT_{\text{treated}} - \Delta CT_{\text{control}}$ . RT-PCRs were run separately for each candidate in triplicate, and data were analyzed for statistical differences by the Mann–Whitney *U* test using PRISM 4.0 software (GraphPad, San Diego).

## **VI. *In vivo* studies of the effects of polyphenol metabolites on NMDA induced retina ganglion cells apoptosis**

Male Sprague-Dawley mice weight 250-300 g were used as experimental animals were divided into 7 groups. There were 3 mice in each group. Drugs with different concentrations were dissolved in 2.5% DMSO in a final volume of 1mg/ml by deep sub-tendon injection to rats (10  $\mu$ l/rat) under anesthesia with pentobarbital (40 mg/Kg). The concentration of each group was listed in Table 1. NMDA and polyphenols were prepared in sterile solution and were injected using a 10 Hamilton syringe with a small needle. The eyes of mice were enucleated 24 h after drugs were given, rats were anaesthetized with pentobarbital and perfused transcardially with 0.9% saline followed by 4% paraformaldehyde in phosphate buffer pH 7.4. The eyes were enucleated and immersed fixed for 1 hour in 4% paraformaldehyde, transferred to 10% neutral-buffered formalin overnight and processed for routine paraffin-embedded sectioning on an automated tissue processor (Shandon Pathcentre, Thermo Shandon Inc., Pittsburgh, PA) Eyes were embedded sagittally and 5  $\mu$ m serial sections are cut with a rotary microtome (Microm HM 330, McBain Instruments, Chatsworth, CA) and stained with hematoxylin and eosin (H&E). The sections were stained for hematoxylin and eosin (H&E) and TUNEL stain (TdT-mediated dUTP nick end labeling). Flat preparations of whole retinas were performed according to a previously described method (138). After anterior segment was removed, the retina was separated from the sclera under a binocular operating microscope on a glass slide with the nerve fiber layer (NFL) facing upward. Several radial cuts were made and the retina was further flattened with a hairbrush. Counting of nuclei was performed according to a previous described method by Kwong and Lam (125). Retina is divided into three areas: superior

peripheral, inferior peripheral and inferior posterior regions. The superior peripheral region was designated 6 mm directly above the center of the optic nerve head. Inferior peripheral and posterior regions were 8 and 2 mm directly below the center of the optic nerve head, respectively. The number of stained nuclei at the RGCs layer was taken under a light microscope with 400×magnification and an eye piece reticule. Three adjacent fields were sampled at each region and the numbers averaged. The number of cells is expressed as percentage of normal control retinas at the corresponding locations.

## **VII. Statistical analysis**

The results were presented as mean  $\pm$  SEM. Statistical significance was determined by one-way analysis of variance (ANOVA) followed by a turkey multiple-comparison test.  $*p < 0.05$  and  $**p < 0.001$  were considered significant for all experiments.

## **Results:**

### **I . Genetic polymorphisms of glaucoma in Taiwan**

#### **(1) Association of E-Cadherin Gene 3'-UTR C/T Polymorphism with POAG**

CDHs play important roles in tissue morphogenesis. Some study suggested that the homeostasis of trabecular meshwork and lamina cribrosa in the optic nerve was out of balance in patients with POAG. Consequently we study the relation of CDH and POAG. All patients were followed up from between 2 to 8 years (average: 5 years). Ten of the patients received trabeculectomy and two of the ten patients underwent trabeculectomy twice at different sites. Fifty patients in the POAG group controlled intraocular pressure by topical drugs. Each patient used an average of 1.3 types of anti-glaucomatous drugs. Nine patients did not require drugs to control IOP following trabeculectomy.

The bands on the gel revealed digested (CC) homozygote, undigested (TT) homozygote and (C/T) heterozygotes (Fig. 1). For quality control, we sequenced the PCR products to define the polymorphism. (Fig. 2a, b and c) The frequencies of the genotypes in the POAG group and the control group are shown in Table 2. The allelic frequency of "C": "T" was 47.6 %: 52.4 % in the control group and 83.3 %: 16.7 % in the POAG group (Table 2). The distribution of the E-CDH gene 3'-UTR C/T polymorphism showed statistical differences in the distribution of genotype frequencies between POAG patients and normal controls ( $p < 0.001$ ). The odds ratio (OR) was significantly different between the normal control and POAG patient groups (OR=5.510, 95 % confidence interval =3.171-9.574) in C allele frequency. The distribution of the C allele was significantly higher in the POAG

group than in the normal control group ( $p < 0.001$ ). The odds ratio was also significant different between two groups in the frequency of the CC and CT genotype, (OR=40.089, 95 % confidence interval = 13.919-115.466). The odds ratio was also significantly different between the two groups in CC and TT genotype (OR=82, 95 % confidence interval = 8.594-782.371). The distribution of the CC homozygote was significantly higher in the POAG group than in the normal control group ( $p < 0.001$ ). OR was still significant when analyzed by methods of regression according to age. We also calculated “power” to test the null hypothesis by SPSS<sup>R</sup>. Under the consideration of genotype CC homozygote, there is a power of 100% to yield a statistically significant result in this sample size (Table 2).

## **(2) The Distribution of Oxidation enzyme eNOS and Myeloperoxidase in POAG**

In the eye, NO regulates the baseline ocular blood flow rate in response to physiological stress (44). A number of studies have indirectly shown that ocular NOS activity may have been increased under physiological stress, e.g. ischaemia (46, 47) and IOP elevation (48, 49). Consequently, we study the relation of NOS and POAG. Using the Fisher’s exact test, we compared the distribution of eNOS into 4 polymorphism between the healthy control and POAG patients. There was no significant difference between two groups. ( $p = 0.481$ ) (Table 3a). The distribution of the genotypes in the control group revealed 0 (0%) a-deletion homozygote, 17 (17.0%) a-deletion and b-insertion heterozygote and 83(83.0%) b-insertion homozygote. The distribution of the genotypes in POAG group revealed 0 (0 %) a-deletion homozygote, 10 (15.4%) a-deletion and b-insertion heterozygote and 56 (84.6%) b-insertion homozygote. The frequency of the each allele (Table 3b) was also no significantly difference. Using the Fisher’s exact test, the distribution of the

eNOS promoter-786 gene polymorphism in the healthy control group and POAG patients was not significantly different. ( $p=0.555$ ) (Table 4a). The distribution of the eNOS promoter-786 genotypes in the control group revealed 84 (82.9%) T/T homozygote, 16 (17.1%) T/C heterozygote and 0(0%) C/C homozygote. The distribution of genotypes in the POAG group revealed 55 (83.3%) T/T homozygote, 11 (16.7%) T/C heterozygote and 0 (0%) C/C homozygote. The frequency of the each allele (Table 4b) was also no significantly difference. Using the Fisher's exact test, the distribution of the MPO -463 G to A gene polymorphism in the healthy control group and the patients group was not evidently different ( $p=0.292$ ) (Table 5). The distribution of genotype of MPO -463 gene polymorphism in the control group revealed 92 (2.0 %) A/A allele homozygote, 27 (27.0 %) A/G allele heterozygote and 71 (71.0 %) G/G allele homozygote. The distribution of MPO -463 genotype are also no significant differences between two group. The results suggest that, no significantly different between the control group and the POAG patients in eNOS intro-4 a-deletion/b-insertion, eNOS promoter-786 T to C polymorphism and MPO -463 G to A gene polymorphism in POAG patients and normal control. Therefore, these polymorphisms are all not useful marker for POAG in Chinese.

## **II. *In vitro* model of glaucoma**

### **(1) The property of N18 RGCs**

The retina ganglion cells expressed antigens specific for photoreceptors, bipolar cells, ganglion cells, and retinal glial cells (Fig. 3). In order to define the N18 cells. N18 cells were stained with Thy-1 (which is specific for ganglion cells) (Sigma Chemical Co. [St. Louis, MO, USA]) and NMDA receptors antibodies. In the immunofluorescein stain, dendritic processes were prominently seen in the



Thy-1 stained (Fig. 4a). The NMDA receptors were prominent in the cells (Fig. 4b).

## **(2) The viability of N18 RGCs after NMDA was added**

Different concentrations NMDA were added to N18 RGCs and the apoptosis of cells was detected in order to select appropriate concentration which could be used in this study. NMDA 100  $\mu$ M was able to induce 69.9% of apoptosis in N18 RGCs, which was suitable for evaluating drug efficiency. It also had good representability in this study (Fig. 5a, b).

## **(3) NMDA-induced apoptosis of N18 RGCs with $Mg^{2+}$ free medium**

The openings of NMDA receptors were blocked by the ions -  $Mg^{2+}$ . Once the  $Mg^{2+}$  ion was removed, the NMDA receptor allowed  $Ca^{2+}$  ions to flow in and the signals would be transduced into downstream molecules. NMDA-induced apoptosis of N18 RGCs was compared with the cell culture medium with and without  $Mg^{2+}$  ions. NMDA receptors could be activated in  $Mg^{2+}$  free medium which had beneficial effects for NMDA actions. Therefore  $Mg^{2+}$  free medium was selected for this study (Fig. 6).

## **III. The effects of polyphenols metabolites on NMDA-induced apoptosis of N18 RGCs**

### **(1) Aloe-emodin metabolites was effective in reducing NMDA-induced apoptosis of N18 RGCs**

Six conjugative polyphenols and 4 well-known neuroprotectors were tested in this study. The neuroprotectors were: Insulin-like growth factor I (IGF-I), IGF-II and Insulin-like growth factor binding protein (IGFBP) which were well-known as

neuroprotectors in neural systems other than retina (86-88). Besides, 1-5-methyl -10,11- dihydro- 5H- dibenzo- (a,b) –cyclohepten -5,10- imine maleate (MK-801; 10  $\mu$ M; Tocris Cookson, Bristol, UK) which was a chemical compound with NMDA antagonist effects was also added as a control group. In the group “base”, only NMDA was added and was used as a positive control group. NMDA 100  $\mu$ M could induce 69.9% apoptosis of N18 RGCs. Among all tested drugs, aloe-emodin metabolites was the most effective one, which could decrease the apoptosis of NMDA-treated N18 RGCs from 69.9% to 50% (\*\* $p < 0.001$ ) which was compatible with MK 801 which could decrease the NMDA-induced apoptosis of N18 RGCs from 69.9 % to 48% (Fig. 7). Consequently, aloe-emodin metabolites was used as the target flavonoid. In the following study, not only the effects of aloe-emodin metabolites but also the signal pathways in reducing NMDA-induced apoptosis in N18 RGCs were all studied.

## **(2) Suitable concentration of aloe-emodin metabolites for reducing NMDA-induced apoptosis of N18 RGCs**

The effects of aloe-emodin metabolites with different concentrations were compared, in order to find out the minimum dosage to achieve the maximum effect. In all mediums except control group 100  $\mu$ M NMDA were added. In control group, only 15  $\mu$ M NMDA was added. In different concentrations of aloe-emodin metabolites, 15  $\mu$ M is most suitable. The concentrations of aloe-emodin metabolites over then 15 $\mu$ M were not more effective than aloe-emodin metabolites with 15  $\mu$ M. Nevertheless, the concentrations of aloe-emodin metabolites less than 15 $\mu$ M were null and void on NMDA-induced apoptosis of N18 RGCs. In control group, only 15  $\mu$ M aloe-emodin metabolites was added. The apoptosis in control group was

identical with the cells without add anything. This proved that 15  $\mu\text{M}$  aloe-emodin metabolites itself had no toxicity on N18 RGCs (Fig. 8).

### **(3) Comparing the effects of parent and metabolites form of aloe-emodin**

Parent and metabolites form of aloe-emodin 15  $\mu\text{M}$  were added individually to N18 RGCs. NMDA 100  $\mu\text{M}$  is also used as an apoptosis inducer in different forms. Besides, MK 801 was added and used as a control again. The conjugative forms of aloe-emodin which was obtained after it is digestive by enzymes is more effective than its parent forms. The aloe-emodin metabolites forms could decrease the apoptosis from 69.9% to 50% but the parent form of aloe-emodin did not have the favorable effects. The parent form of aloe-emodin could only decrease apoptosis of N18 RGCs from 69.9% to 62% (Fig. 9).

### **(4) Detecting the change of $\text{Ca}^{2+}$ concentration after aloe-emodin metabolites adding to NMDA-treated RGCs**

Upon the NMDA receptor was activated,  $\text{Ca}^{2+}$  influx into cells changed the free radicals in cells and involved in cell death. We detected  $\text{Ca}^{2+}$  concentration in different situations. BAPTA is a  $\text{Ca}^{2+}$  chelator. The effects of aloe-emodin metabolites in reducing  $\text{Ca}^{2+}$  is equal to the effects of BAPTA ( $p > 0.05$ ). Aloe-emodin metabolites blocked NMDA-induced cell death might through decreasing the concentration of  $\text{Ca}^{2+}$  (Fig. 10).

## **IV Detecting the apoptosis pathway of aloe-emodin metabolites and NMDA-treated N18 RGCs**

### **(1) The effects of aloe-emodin metabolites was equal to caspase-3 blocker in aloe-emodin metabolites and NMDA-treated N18 RGCs**

Glaucoma was a complex disease. Regardless of the mechanism, however, the ganglion cells ultimately die, a process that represented the common final pathway to glaucomatous vision loss (4, 5). Several studies have demonstrated that RGCs died during development and in a variety of optic nerve diseases by a form of cell death known as apoptosis. NMDA-induced RGCs lost were also in “apoptosis” form. Caspase 3 is the last common step of diverse pathways of cells apoptosis, consequently the effect of aloe-emodin metabolites and caspase 3 blocker on NMDA-induced apoptosis of N18 RGCs was compared. Z-VAD-fmk was a commercial product of caspase-3 activity blocker. The effect of aloe-emodin metabolites on NMDA-induced apoptosis of N18 RGCs was compatible with the effect of Z-VAD-fmk in decreasing apoptosis of N18 RGCs. This data show that aloe-emodin metabolites effects in blocking NMDA-induced cell death through apoptotic pathway (Fig. 11).

### **(2) Aloe-emodin metabolites decreased apoptosis of NMDA-treated N18 RGCs by intrinsic apoptosis pathway**

To clarify the mechanism of aloe-emodin metabolites, the proteins involved in apoptosis pathway were determined by Western blot. The results revealed that NMDA increased the expression of p53 and bax (Fig. 12a-1 and 12a-2), decreased the mitochondrial membrane potential (Table 7) and the expression of caspase 9, but not caspase 8 (Fig 12a-1 and 12a-2), whereas aloe-emodin metabolites rescued their functions (Fig. 12a-1 and 12a-2) ( $p < 0.05$ ). There were no significant changes in caspase 8 (data not shown). Moreover, to clarify the mechanism of aloe-emodin metabolites on NMDA treated N18 RGCs was through intrinsic apoptosis pathway

(Fig. 12b), the change of mitochondrial membrane potential was evaluated and showed a significant increase after the addition of aloe-emodin metabolites (Table 7) ( $p < 0.05$ ) and a significant decrease the mitochondrial membrane potential upon the addition of NMDA.

#### **V. Aloe-emodin metabolites was also effective in decreasing NMDA-induced apoptosis on N18 RGCs *in vivo***

Drugs with different concentrations were delivered 5  $\mu$ l/mice (250g) by deep sub-tendon injection under anesthesia with pentobarbital (40 mg/Kg). The eyes were enucleated 24 hours after drugs were given and histologic examinations were done. The histologic slides showed that: 15  $\mu$ M of aloe-emodin was able to suppress NMDA-induced apoptosis in retinal ganglion cells *in vivo* (Fig. 13a-d) (H&E 40 $\times$ 10). 5 $\mu$ M of aloe-emodin cannot suppress NMDA-induced apoptosis in retinal ganglion cells *in vivo* (Fig. 13-e). The nucleus of ganglion cells became irregular and fragmented (Fig. 13-g). Aloe-emodin itself did not have toxicity to RGCs *in vivo*. (Fig. 13-b) Deep sub-tendon injection was a good and safe method to deliver aloe-emodin to eyes (Fig. 13-f). The average number of RGCs was from 3 area of the retina calculated by the method stated in the section of "Materials and Methods" and results showed that the number of RGCs of aloe-emodin treatment group was significantly higher than NMDA alone group (Table 8). Besides, the TUNEL positive cells in aloe-emodin and NMDA-treated were also less than only NMDA-treated N18 RGCs. (Fig. 13-h and i, Table 8)

#### **VI. Aloe-emodin metabolites decreased NMDA-induced apoptosis of RGCs by increasing of Cu-Zn superoxide dismutase**

## **(1) The proteins changed in NMDA and aloe-emodin metabolites treated N18 RGCs**

The 2D-PAGE was a 17 cm strip and immobilized to pH 3-10 IPG strip. Protein spots from each gel were detected and matched automatically. The intensity of the spots was compared among gels. Thirty-three spots were selected at first, they existed only in aloe-emodin metabolites and NMDA co-treated group, and absent in the negative control or only NMDA-added group (the expression of the 33 proteins were induced by aloe-emodin metabolites) (Fig. 14). Furthermore, 51 spots were expressed both in the control and in the aloe-emodin metabolites-treated group, but were not expressed in the NMDA-treated group (the expressions of the 51 proteins were preserved from original condition even NMDA and aloe-emodin metabolites were added to the N18 RGCs) (Fig 15). In gel digestion and nano-LC-MS/MS analysis were processed for gel pieces from 84 spots labeled in Fig. 17 and Fig. 18. The I.D. of 84 protein spots listed in table 12. All identifications were manually validated by taking into account the MOWSE score, apparent versus predicted isoelectric points and molecular weights, as well as the error distribution of apparent versus predicted peptide masses ( $m/z$ ).

## **(2) The proteins related to neuroprotection**

The focus of this study was placed on the proteins involved in the defense of oxidation, stress and apoptosis. The selective criterion of the proteins was that the expression of proteins had to be 2-fold the differential expressions (Table 9). The distributions of involved proteins were as follows and listed in Fig. 16: Stress-evoked proteins: 7.8%; Proteins involved in cell growth: 6.3%;

Housekeeping proteins: 23.4%; Proteins involved in production of energy in cells: 31.3%; Proteins involved in formation of cell structures: 14.1%; Miscellaneous proteins: 17.2%. Among the 84 spots, we identified 9 proteins for further study. There were two stress-evoked proteins, two proteins involved in cell growth, three proteins involved in production of energy, and two proteins relate to the formation of cells' structures (Table 10). Based on nano-LC-MS/MS, these spots (spots 2, 4, 15, 19, 21, 24, 32, 34, 44) (Fig. 17) were identified. Their nano-LC-MS/MS spectra are shown in Fig. 20a-i, respectively. Tryptic peptides from these spots matched those predicted for these proteins. Their positions on the 2-DE gel are in agreement with the theoretical pIs and M.W.s, respectively. The proteins were characterized as galectin-1, elongation factor 1-beta (EF 1- $\beta$ ), 60 kDa heat shock protein (Hsp 60) , stress-70 protein, superoxide dismutase [Cu-Zn] (Cu-Zn SOD), 10 kDa heat shock protein (Hsp 10), voltage-dependent anion-selective channel protein 1 (VDAC-1), mitochondrial inner membrane protein (Mitofilin) and protein disulfide-isomerase (PDI) A6 precursor. Of these proteins, galectin-1, EF 1- $\beta$ , Hsp 60, stress-70 protein, Cu-Zn SOD, Hsp 10 and VDAC-1 were prominently expressed only when aloe-emodin metabolites were added to the N18 RGCs and were not expressed in the control group, indicating that these proteins were induced by aloe-emodin metabolites. Mitofilin and PDI A6 precursor were expressed significantly both in the control and aloe-emodin metabolites co-treated N18 RGCs. This meant that Mitofilin and PDI A6 precursor were naturally expressed in N18 RGCs and acted as elements in the function of neuroprotection.

### **(3) The RNA expressions of the neuroprotective-proteins**

The RNA expressions of nine proteins obtained from various treatments were assayed by real-time Q-PCR (Table 9). The RNA expression in RGCs with

and without the addition of aloe-emodin metabolites was compared. The primer sequences and reactive conditions were listed in the Table 11. The results were normalized to the level of GAPDH (a housekeeping gene). The Q-PCR results revealed that the RNA levels of Cu-Zn SOD, Hsp10 and PDI A6 precursor increased in NMDA-treated RGCs, whereas those of galectin-1, EF 1- $\beta$ , Hsp 60, stress-70 protein, VDAC-1 and Mitofilin decreased (Table 12). Furthermore, other than the RNA levels of galectin-1 ( $p=0.025$ ) and Mitofilin ( $p=0.020$ ), EF 1- $\beta$ , Hsp 60, stress-70 protein, VDAC-1 and PDI A6 precursor decreased upon addition of aloe-emodin metabolites but did not reach statistical significance ( $p>0.05$ ) (Table 12). The results were not in good agreement with the protein expressions revealed in 2-DE gel. Several post-translational modifications, including phosphorylation, glycosylation and degradation, which are aberrantly regulated in many diseases may also interfered the results of this study, the changes of the proteins in the study cannot be predicted by measuring the amount of mRNA. Therefore, post-translational modifications of these proteins were also analyzed by nano-LC-MS/MS. Some post-translational modifications were identified in Hsp 60, stress-70 protein, VDAC-1 and PDI A6 precursor. Hsp 60 was oxidized at M55, M256 and M177, stress-70 protein was deamidized at N268, VDAC-1 was deamidized at N61 and PDI A6 precursor was oxidized at M326, M358 and M427 (Fig. 17 A-I). The phenomena of post-translational modifications might have influenced the function of the proteins resulting in the non-parallel expressions of proteins and RNA. On the other hand, the RNA expressions of Cu-Zn SOD, Hsp 10 and PDI A6 were up-regulated by aloe-emodin metabolites, which was consistent with the protein levels of the proteins obtained by 2DE gel. Nevertheless, only the range of increasing of Cu-Zn SOD had significant difference ( $p=0.01$ ) (Table 12) in the expressions of RNA, the increased expression of Hsp 10 and PDI A6 after



adding aloe-emodin metabolites were not significantly different ( $p > 0.05$ ) (Table 12). The expression of the three proteins were also detected by Western blot and revealed correlated results (Fig. 18a and 18b) In table 10, the results of Q-PCR revealed that there were significant differences in Galectin-1, Cu-Zn SOD and Mitofilin. Nevertheless, only the RNA level of Cu-Zn SOD was increasing which was consistent with the data of proteomics.

## **Discussion**

### **I . Genetic polymorphisms in glaucoma patients**

#### **(1) E-Cadherin gene 3'-UTR C/T polymorphism was marker for POAG in Taiwan**

Cell-cell adhesion plays essential roles in organogenesis, physical transport, signal transmission and immunological function in multicellular organisms. CDHs are single-pass transmembrane glycoproteins that associate as cis-dimers on the cell surface and then combine to form a linear zipper-like structure which promotes homophilic intercellular adhesion. MMP is required for the efficient cleavage of E-CDH during apoptosis. In this study, the “C” allele [(C allele was significantly higher in the POAG group than in the normal control group ( $p<0.001$ ) and “CC” genotype are useful markers for Chinese POAG of E-CDH gene –3’-UTR gene polymorphism “CC” homozygote was significantly higher in the POAG group than in the normal control group ( $p<0.001$ ). We suspect this allele disturbs the effect of E-CDH in trabecular meshwork and even the lamina cribrosa of optic nerve head. Moreover, the disturbed effects of E-CDH may change the balance of E-CDH and matrix metalloproteinases (MMP), such cause the unbalance of aqueous humour outflow in trabecular meshwork and change the resistances of lamina cribrosa of glaucomatous optic nerve. Besides, E-CDH itself has a close relationship with apoptosis, which also play important mechanisms in the onset and progression of POAG. The roles of genetic polymorphism may include direct causation, linkage disequilibrium, natural selection and population stratification. Therefore, we are not going to conclude that “C” allele of E-CDH gene –3’-UTR gene polymorphism is the direct cause of POAG, we can just indicate there is an association. As we know,

3'-UTR is not the translated area of protein, the exact role of E-CDH plays in the development of POAG is unknown and other factors may be added to explain the effects of "C" allele gene polymorphism on POAG. The understanding about E-CDH gene 3'-UTR is limited. Keirsebilck A had proposed that E-CDH 3'-UTR sequence may trigger the mRNA instability and downregulation of E-CDH expressed in mesenchymal tumor cells (119, 126). But there are many examples in some genes that the 3'-UTR may change the expression of genes. Such as p53 3'-UTR that contains an Alu-like repetitive element and a deletion of the distal end of the p53 3'-UTR increased the efficiency of translation (127). Besides, 3'-UTR is also critical for cAMP-mediated Na (+)-coupled glucose co-transporter SGLT1 message stabilization (127). Consequently, the exact role of "C" allele of E-CDH gene –3'-UTR gene polymorphism need to be resolved by advanced studies such as "proteomics", that is, the post translated products of the gene and the protein-protein interaction of the gene related proteins may be needed to sole this question in the future.

## **(2) The distribution of oxidation enzyme eNOS and myeloperoxidase in POAG**

NO isoenzymes have been identified in all regions of the eye (128). NOS is evident in the major sites of outflow resistance (trabecular meshwork and Schlemm's canal), in collecting channels and particularly in the ciliary muscle (129). NO is an important mediator of the homeostatic functions of the eye, including regulation of aqueous humour dynamics, neuronal visual processing, local modulation of ocular blood flow and control of retinal ganglion cell death by apoptosis (144). Information on the NOS system in human eyes is limited.

Nathanson in 1993 (129) and Schuman in 1994 (130) proposed that topical or intracameral application of NO donors can alter the aqueous humour outflow facility in rabbits and monkeys. A deficit in NOS-like immunoreactivity has been found in the ciliary muscle and outflow pathway in primary open-angle glaucoma (131, 132). NO levels in the aqueous humour have been found to be higher in glaucoma patients than in cataract patients, but NO levels vary significantly in different types of glaucoma (133). Concentrations of cGMP in the aqueous humour in normal-pressure glaucoma patients have been found to be lower than those in control patients (134). Chronic overproduction of NO has been associated with neuronal degeneration, such as Parkinson's disease and Alzheimer's disease (135). The retina is an extension of the central nervous system, it has a very high poly-unsaturated fatty acids (PUFA) content and is susceptible to oxidative damage (136). NO can either attack the double bonds on the membrane PUFA (136) or modify the genetic nuclear materials (137), causing necrotic and apoptotic cell death. The detailed mechanism of how the retinal NOS activity is regulated under elevated IOP remains unclear. Further studies are required to elucidate the retinal NO regulatory mechanism under elevated IOP through different NOS sub-groups. Selective inhibition of NOS caused conflicting results in neuronal protection studies. For example, introduction of N<sup>G</sup>-nitro-L-arginine (L-NNA) to a retinal ischaemic animal model demonstrated both worsening (138) and protective effects. That is to say small amount of NO production is beneficial to the retina as it can up-regulate the blood circulation and thus facilitates the flow of metabolites. Excessive NO, however, may damage the retinal tissues (139) by a free radical oxidative mechanism (140). As for NO and MPO genes study in POAG patients are still in the spouting period and many efforts still may be done in this field. Before the roles of NO are fully characterized, the application of NOS inhibitor in glaucoma (141,

142) remains experimental. Meanwhile, preventive strategy (such as anti-oxidative supplements) may complement the stringent control of IOP to combat the glaucoma-related oxidative stress. The potential applications of antioxidants in retinal therapy deserve further attention. Although in present study our candidate genes polymorphisms are no useful markers for POAG patients. Nevertheless we are going to investigate the roles of other free radicals related genes in POAG patients and the proteomics views of free radicals in RGCs under glaucoma stress.

The most mentioned genes about POAG are myocilin (MYOC) gene (chromosome position 1q23-q24) and optineurin gene (chromosome position 10p13). The pathophysiology of POAG is not precisely known. POAG is a multifactorial disease (143, 144), and the assumption that a single gene is involved is not reasonable. POAG may be the result of multiple and interactive genetic and environmental effects. There is a recognized increased risk of developing the disease in family members of patients with POAG. Currently, there is a lack of information regarding the genetics of the disease and, hence, the molecular biology of glaucoma is currently under close investigation. Although in present study our candidate genes polymorphisms are no useful markers for POAG patients. The exact role of NOS genes need to be resolved by advanced studies such as other gene polymorphisms, the post translated products of the gene and the protein- protein interaction of the gene products may solve this question. Single nucleotide polymorphisms (SNPs) have important implications in human genetic studies. The screening for such alleles helps in the detection of a genetic predisposition to disease. The presence of a specific SNP allele can be implicated as a causative factor of a genetic disorder. Besides, understanding the associated polymorphism is expected to increase the understanding of the course of disease. Knowing the genetic role of POAG was important for designing new treatments for glaucoma.

## **II. Aloe-emodin metabolites was effective in decreasing apoptosis of NMDA-induced N18 RGCs**

Aloe-emodin is an anthraquinone polyphenol present mainly as glycosides (aloe-emodin parent form) in Chinese herbs, like *Rheum palmatum* and *Aloe vera*. Aloe-emodin parent form has been shown to possess neuroprotection, antioxidation, anti-inflammatory and anticancer effects (145). However, in recent years, controversies abound concerning which forms of polyphenols are actually absorbed: glycoside, aglycone, or both forms. Polyphenol glycosides are generally hydrophilic and thus cannot be transported across membranes by passive diffusion. Upon hydrolysis by the enzymes released by enterobacteria, the sugar moieties of polyphenol glycosides are cleaved, resulting in more lipophilic aglycones, which become permeable through the gut wall. The polyphenol aglycones are further metabolized into sulfates and glucuronides (146-149). Therefore, in this study, conjugated metabolites of aloe-emodin (aloe-emodin s/g) prepared from rat serum, the exact forms circulating in blood, was tested for their neuroprotective effect on NMDA-induced apoptosis of RGCs. Among the candidates tested, aloe-emodin metabolites was the most effective and even more potent than the known neuroprotectors. Overactivation of NMDA receptors led to toxic  $\text{Ca}^{2+}$  overloading (150, 151) and the known neuroprotective agents could decrease the NMDA-induced  $\text{Ca}^{2+}$  overloading. Aloe-emodin metabolites at the concentration 15  $\mu\text{M}$  was found to decrease the  $\text{Ca}^{2+}$  concentration and reduced NMDA-induced apoptosis of RGCs. The effect of aloe-emodin s/g was almost equal to the results from the caspase 3 blocker and  $\text{Ca}^{2+}$  chelator. Therefore, aloe-emodin was a potential candidate of neuroprotector in glaucomatous neuropathy.

### **III. Aloe-emodin metabolites regulated NMDA-treated N18 RGCs by intrinsic apoptosis pathway**

In general, apoptosis was activated by two main pathways: the receptor-mediated pathway and the intrinsic (mitochondrial) pathway. Components of the FAS/FAS ligand system represent the prototypical receptor-mediated apoptosis pathway (152). Intrinsic pathway did not involve a surface receptor, but rather was formed by the modification of intracellular pools of proteins. Environmental or intracellular stressors resulted in post-translation modification of proteins in intrinsic pathway, which then exerted their effect on the mitochondria to release cytochrome c. The released cytochrome c then bound with apoptosis-activating factor-1 and caspase-9 to form a complex known as the apoptosome, which in turn activates more downstream apoptotic reactions. Aloe-emodin metabolites suppressed the NMDA-induced apoptosis of N18 RGCs cells by decreasing the expression of caspase 9 but not caspase 8, implying the modulation was by way of intrinsic (mitochondrial) pathway.

### **IV. Aloe-emodin was effective in decreasing apoptosis of N18 RGCs *in vivo***

Sub-tendon injection is an universal technique in general ophthalmic practice. NMDA and various doses of aloe-emodin were administered to mice via sub-tendon injection. The toxicity of NMDA and neuroprotective effects of aloe-emodin in mice eyes were examined histologically and the results further confirmed those effects of aloe-emodin on RGCs culture. Aloe-emodin was not toxic to RGCs *in vivo* and was useful in decreasing NMDA-induced RGCs apoptosis. Sub-tendon injection was a good and safe method to deliver aloe-emodin to eyes.

## **V. Aloe-emodin metabolites decreased apoptosis of NMDA-treated RGCs by Cu-Zn SOD**

Proteomics has been successfully used to compare changes in protein levels that happen in a wide range of diseases (153, 154). In this study, we applied this technique to detect the mechanisms by which aloe-emodin metabolites acted as the neuroprotector in NMDA-treated N18 RGCs. By comparing the differences in protein profile patterns between treatments with and without aloe-emodin metabolites in NMDA-treated N18 RGCs, we detected that some proteins were expressed in different amount. The primer sequences and reactive conditions were listed in the Table 11. The results indicated that proteins involved in the regulation of energy in cells were the most prominent group to be affected by aloe-emodin metabolites and occupied 31.3%. Other proteins affected by aloe-emodin metabolites included those involved in cells' growth, formation of cells' structures and stress-induced proteins which regulate intracellular function. These proteins might exert protective effects to decrease apoptosis of NMDA-treated N18 RGCs. Of the detected proteins, Galectin-1 (155), EF 1- $\beta$  (156), Hsp 60 (157), stress-70 protein (157), Cu-Zn SOD (158), Hsp 10 (157) and VDAC-1 (159) were prominently expressed only when aloe-emodin metabolites were added and absent in control group, indicating that they were induced by aloe-emodin metabolites and associated with neuroprotection. The physiology function of Galectin-1 is as an autocrine negative growth factor that regulates cell proliferation (Table 10) (156). From the data generated by Q-PCR (Table 10 and Table 12), galectin-1 was down-regulated upon the addition of aloe-emodin metabolites. The result from Q-PCR but not the results from proteomics conformed to the physiology function of galectin-1 which is a negative growth factor. The expressions of RNA and protein in



galectin-1 were not equal. Nevertheless, there was no post-translation modification detected and the diverse expression of RNA and protein in galectin-1 may be due to other influences, such as protein-protein interaction. EF-1 was reported to stimulate the exchange of GDP bound to EF-1-alpha to GTP and to affect the GDP/GTP exchange (156), which is closely related to the activity and life-span of cells. The functions of Hsp 60, stress-70 protein and Hsp 10 have been reported to be involved in mitochondrial protein import, control of cell proliferation, cellular aging and to possibly act as a chaperone (157). Hsp 60, stress-70 protein and Hsp 10 were often up-regulated when conflicted with stress. In this study, the results of Q-PCR revealed that the RNA of EF-1-alpha, Hsp 60 and stress-70 were down-regulated in aloe-emodin metabolites added RGCs; this result was not identical to the expressions in the 2-DE gel and did not conform to their physiologic functions. The discrepancy in expression of Hsp 60 and stress-70 might have resulted from the post-translational modifications of these proteins, because Hsp 60 was oxidized at M55, M256 and M177 and stress-70 protein was deamidized at N268. Post-translational modification of proteins may affect the function of proteins and change the fate of cells and this may explain the different expression of these proteins from the results of proteomics and Q-PCR. Regarding to EF-1-alpha, there were no post-translational modification detected in it; determining the exact role of EF-1-alpha will require further investigation. Hsp 10 was up-regulated upon aloe-emodin metabolites addition; this result was identical to its expression in the 2-DE gel and conformed to its physiologic function. Nevertheless, there was no significant difference in the expression of RNA level of Hsp 10. Cu-Zn SOD has been shown to destroy radicals and to be an important molecule in antioxidation (158). The results of Q-PCR revealed that the RNA level of Cu-Zn SOD was up-regulated by aloe-emodin metabolites and showed statistical difference; this was

consistent with its expression in the 2-DE gel and its physiologic function. The expression of Cu-Zn SOD was most affirmable in all the proteins analyzed in this study. The RNA level of VDAC-1 was down-regulated by NMDA and further down-regulated by aloe-emodin metabolites. VDAC-1 has been reported to form a channel through the mitochondrial outer membrane as well as the plasma membrane (159). Besides, Mitofilin is a mitochondrial inner membrane protein (160); it plays an important role in the apoptosis process and in the changing of mitochondrial membrane potential. The expressions of the protein levels of VDAC-1 and Mitofilin were not identical to that of 2-DE gel. There are diverse functions of VDAC-1 and Mitofilin, the expressions of the proteins could not be predicted. There was no reasonable explain about the expressions of RNA and protein levels of VDAC-1 and Mitofilin now and need advanced investigation. PDI A6 precursor functions in the rearrangement of S-S bonds in proteins (161). The RNA level of PDI A6 precursor was up-regulated by aloe-emodin metabolites, which was consistent with the result of 2-DE. Nevertheless the results did not have statistical difference. Several post-translational modifications of PDI A6 precursor at M326, M358 and M427 with oxidation were detected but the oxidative modification often did not interfere with its protein expression. The reasonable reason about the diverse expressions of the levels of RNA and protein of PDI A6 also need advanced investigation.

We had identified some proteins involved in the neuroprotection effects of aloe-emodin metabolites. These proteins were associated with the regulation of energy, apoptosis and oxidation in cells. In conclusion, the effects of aloe-emodin metabolites on the NMDA-treated RGCs were closely associated with the regulation of apoptosis and antioxidation. Nevertheless, the results of RNA level were not completely consistent with those of 2-DE gel. We hypothesized that this

may due to the occurrence of instability of mRNA, protein-protein interaction during translation or post-translation modifications. Besides, the global condition was not the same before and after NMDA and aloe-emodin metabolites were added might influence the expression of the protein. It is important to take the protein expression and RNA levels together in order to view the mechanism and pathways of the reaction in the study. Among the studied molecules, RNA and protein expressions of Cu-Zn SOD, Hsp 10 and PDI A6 were identical. In the three proteins, only the RNA level of Cu-Zn SOD had significant difference after aloe-emodin metabolites was added (Table 10) and this result was also proved by Western blotting (Fig. 18a and 18b). Cu-Zn SOD may be a very important molecule in the pathway of aloe-emodin metabolites in reducing apoptosis in NMDA-treated N18 RGCs. We supposed that 15  $\mu\text{M}$  of aloe-emodin metabolites by way of scavenging free radical effect of Cu-Zn SOD protected NMDA-treated N18 RGCs. The exact effects of Cu-Zn SOD may need advanced investigation to understand its whole role. But this did not mean that other proteins detected by 2-DE gel and nano-LC-MS/MS analyses were not important. These proteins might also involve in the mechanisms of the reaction of aloe-emodin metabolites, but they needed further studies to prove their effects. Besides, glutamate cytotoxicity may not be the issue of acute rise in IOP (162). Consequently, we will test the effects of aloe-emodin metabolites and proteins involved in different stresses induced apoptosis in N18 RGCs in the future. Under pathological conditions, chronic low-grade overactivation of the NMDA receptor causes an excessive amount of  $\text{Ca}^{+2}$  influx into the nerve cell which then triggers a variety of processes that can lead to apoptosis. Overloading of  $\text{Ca}^{+2}$  will result in the formation of oxygen free radical. Overloading of  $\text{Ca}^{+2}$  activates neuronal nitric oxide synthase (NOS), increases production of nitric oxide (NO) and the formation of toxic peroxynitrite (ONOO<sup>-</sup>).

These changes activate transcription factors that can go into the nucleus and influence neuronal injury and apoptosis. Consequently, NMDA-induced apoptosis in RGCs could be suppressed by aloe-emodin through regulating the antioxidant, Cu-Zn SOD, was a trustful result. Aloe-emodin metabolites was a potential agent for neuroprotective therapy for glaucomatous patients by destroying radicals to reduce apoptosis in RGCs.

## **Conclusion:**

In SNPs study of glaucoma, we had found the useful genetic marker for POAG patients in Taiwan and this might help us in predicting the susceptibility of POAG and design new treatment of the disease. Halpotype study of the related alleles and fuctional studies of these SNPs in the future may help us understand the disease in advanced.

Aloe-emodine was a useful neuroprotector in an *in vitro* glaucoma model and in *in vivo* study. The reaction was through intrinsic apoptoisis pathway. In oxidative reaction, Cu-Zn SOD which was a powerful antioxidant helped aloe-emodin metabolites in protecting NMDA-treated N18 RGCs. In the future, phase II to phase III must be done before it can be used in clinical practice.



## References

1. Quigley HA. Number of people with glaucoma worldwide. *Br J Ophthalmol* 1996;80:389-403.
2. Shields MB, Ritch R, Krupin T. Classification of the glaucomas. In: *The glaucoma*. St Louis: Mosby-Year Book Inc, 1996;2:717-725.
3. Wolfs RC, Borger PH, Ramrattan RS, Klaver CC, Hulsman CA, Hofman A, Vingerling JR, Hithings RA, de Jong PT. Changing views on open-angle glaucoma: definitions and prevalences—The Rotterdam Study. *Invest Ophthalmol Vis Sci* 2000;41:3309-3321.
4. Garcia Valenzuela E, Gorczyca W, Darzynkiewicz Z, Sharma SC. Apoptosis in adult retinal ganglion cells after axotomy. *J Neurobiol* 1994;25:431-438.
5. Garcia-Valenzuela E, Shareef S, Walsh J, Sharma SC. Programmed cell death of retinal ganglion cells during experimental glaucoma. *Exp Eye Res* 1995;61:33-44.
6. Sommer A, Tielsch JM, Katz J, Quigley HA, Gottsch JD, Javitt J, Singh K. Relationship between intraocular pressure and primary open angle glaucoma among white and black Americans. The Baltimore Eye Survey *Arch Ophthalmol* 1991;109:1090-1095.
7. Kirwan RP, Crean JK, Fenerty CH, Clark AF, O'Brien CJ. Effect of cyclical mechanical stretch and exogenous transforming growth factor-beta1 on matrix metalloproteinase-2 activity in lamina cribrosa cells from the human optic nerve head. *J Glaucoma* 2004;13:327-334.
8. Fingert JH, Heon E, Liebmann JM, Yamamoto T, Craig JE, Rait J, Kawase K, Hoh ST, Buys YM, Dickinson J, Hockey RR, Williams-Lyn D, Trope G,

- Kitazawa Y, Ritch R, Mackey DA, Alward WL, Sheffield VC, Stone EM. Analysis of myocilin mutations in 1703 glaucoma patients from five different populations. *Hum Mol Genet* 1999;8:899-905.
8. Klemetti A. Low-tension glaucoma--a disease for ophthalmology or internal medicine? *Duodecim* 1997;113:1425-1426.
  9. Stuart JM, Glaucoma, apoptosis, and neuroprotection. *Current Opinion in Ophthalmology* 1997;8:28-37.
  10. Stone EM, Fingert JH, Alward WL, Nguyen TD, Polansky JR, Sunden SL, Nishimura D, Clark AF, Nystuen A, Nichols BE, Mackey DA, Ritch R, Kalenak JW, Craven ER, Sheffield VC. Identification of a gene that causes primary open angle glaucoma. *Science* 1997;31:275:668-670.
  11. Ortego J, Escribano J, Coca-Prados M. Cloning and characterization of subtracted cDNAs from a human ciliary body library encoding TIGR a protein involved in juvenile open angle glaucoma with homologous toneyosin and olfactomodulin. *FEBS Lett* 1997;413:349-353.
  12. Kubota R, Noda S, Wang Y, Minoshima S, Asakawa S, Kudoh J, Mashima Y, Oguchi Y, Shimizu N. A novel myosin-like protein (myocilin) expressed in the connecting cilium of photoreceptor molecular cloning, tissue expression, and chromosomal mapping. *Genomica* 1997;41:360-370.
  14. Lin HJ, Tsai CH, Tsai FJ, Chen WC, Chen HY, Fan SS. Transporter associated with antigen processing gene 1 codon 333 and codon 637 polymorphisms are associated with primary open angle glaucoma. *Mol Diagn* 2004;8:245-252.
  15. Lin HJ, Tsai SC, Tsai FJ, Chen WC, Tsai JJ, Hsu CD. Association of interleukin 1 beta and receptor antagonist gene polymorphism with primary open angle glaucoma. *Ophthalmologica* 2003;217:358-364.

16. Lin HJ, Tsai FJ, Chen WC, Chi YR, Hsu Y, Tsai SW. Association of tumor necrosis factor alpha-308 gene polymorphism with primary open angle glaucoma in Chinese. *Eye* 2003;17:31-34.
17. Lin HJ, Chen WC, Tsai FJ, Tsai SW. Distribution of p53 codon 72 gene polymorphism with primary open angle glaucoma. *Br J Ophthalmol* 2002;86:771-773.
18. Drance SM, Schulzer M, Thomas B, Douglas GR. Multivariate analysis in glaucoma use of discriminant analysis in predicating glaucomatous visual field damage. *Arch Ophthalmol* 1981;6:1019-1022.
19. Laske MC, Connell AMS, Wu S, et al. Risk factor of open-angle glaucoma. *Arch Ophthalmol* 1995;113:918-924.
20. Tsai FJ, Lin HJ, Chen WC, Tsai CH, Tsai SW. A codon 31ser-arg polymorphism of the WAF-1/CIP-1/p21/tumour suppressor gene in Chinese primary open-angle glaucoma. *Acta Ophthalmol Scand* 2004;82:76-80.
21. Tsai FJ, Lin HJ, Chen WC, Chen HY, Fan SS. Insulin-like growth factor-II gene polymorphism is associated with primary open angle glaucoma. *J Clin Lab Anal* 2003;17:259-263.
22. Camras CB, Alm A, Watson P, Stjernschantz J. Latanoprost, a prostaglandin analog, for glaucoma therapy. Efficacy and safety after 1 year of treatment in 198 patients. Latanoprost Study Groups. *Ophthalmology* 1996;103:1916-24.
23. Kuniyasu H, Ellis LM, Evans DB, Abbruzzese JL, Fenoglio CJ, Bucana CD, Cleary KR, Tahara E, Fidler IJ. Relative expression of E-cadherin and type IV collagenase genes predicts disease outcome in patients with resectable pancreatic carcinoma. *Clin Cancer Res* 1999;5:25-33.
24. Nawrocki-Raby B, Gilles C, Polette M, Martinella-Catusse C, Bonnet N, Puchelle E, Foidart JM, Van Roy F, Birembaut P. E-Cadherin mediates MMP



- down-regulation in highly invasive bronchial tumor cells. *Am J Pathol* 2003;163:653-661.
25. Streuli CH, Bailey N, Bissell MJ. Control of mammary epithelial differentiation: basement membrane induces tissue-specific gene expression in the absence of cell-cell interaction and morphological polarity. *J Cell Biol* 1991;115:1383-1395.
26. Yap AS. The morphogenetic role of cadherin cell adhesion molecules in human cancer: a thematic review. *Cancer Invest* 1998;16:252-261.
27. Steinhilber U, Weiske J, Badock V, Tauber R, Bommert K, Huber O. Cleavage and shedding of e-cadherin after induction of apoptosis. *J Biol Chem* 2001;276:4972-4980.
28. Takeichi M. Cadherin cell adhesion receptors as a morphogenetic regulator. *Science* 1991;251:1451-1455.
29. Gumbiner BM. Cell adhesion: the molecular basis of tissue architecture and morphogenesis. *Cell* 1996;84:345-357.
30. Shapiro L, Fannon AM, Kwong PD, Thompson A, Lehmann MS, Grubel G, Legrand JF, Als-Nielsen J, Colman DR, Hendrickson WA. Structural basis of cell-cell adhesion by cadherins. *Nature* 1995;374:327-337.
31. Huber O, Bierkamp C, Kemler R. Cadherins and catenins in development. *Curr Opin Cell Biol* 1996;8:685-691.
32. Vleminckx K, Kemler R. Cadherins and tissue formation: intergrating adhesion and signaling. *Bioessays* 1999;21:211-220.
33. Yap AS. The morphogenetic role of cadherin cell adhesion molecules in human cancer: a thematic review. *Cancer Invest* 1998;16:252-261.
34. La Rosa, Francis A, Lee David A. Collagen degradation in glaucoma: will it gain a therapeutic value? *Curr opin in ophthalmol.* 2000;11:90-93

35. Ando H, Twining SS, Yue BY, Zhou X, Fini ME, Kaiya T, Higginbotham EJ, Sugar J. MMPs and proteinase inhibitors in the human aqueous humor. *Invest Ophthalmol Vis Sci* 1993;34:3541-3548.
36. Samples JR, Alexander JP, Acott TS. Regulation of the levels of human trabecular matrix metalloproteinases and inhibitor by interleukin-1 and dexamethasone. *Invest Ophthalmol Vis Sci* 1993;34:3386-3395.
37. Yan X, Tezel G, Wax MB, Edwards DP. Matrix metalloproteinases and tumor necrosis factor  $\alpha$  in glaucomatous optic nerve head. *Arch Ophthalmol* 2000;118:666-673.
38. Moll R, Mitze M, Frixen UH, Birchmeier W. Differential loss of E-cadherin expression in infiltrating ductal and lobular breast carcinomas. *Am J Pathol* 1993;143:1731-1742.
39. Berx G, Cleton-Jansen A-M, Nollet F, de Leeuw WJ, van de Vijver M, Cornelisse C, van Roy F. E-cadherin is a tumor/invasion suppressor gene mutated in human lobular breast cancer. *EMBO J* 1995;14:6107-6115.
40. Bscker KF, Reich U, Schott C, Hufler H. Single nucleotide polymorphisms in the human E-cadherin gene. *Hum Genet* 1995;96:739-740.
41. Alm A. Ocular circulation. In Adler's *Physiology of the Eye*, Hart, W.M., ed. Mosby St. Louis: MO, U.S.A. 1992:198-227.
42. Dawson, T.M. and Snyder, S.H. Gases as biological messengers: nitric oxide and carbon monoxide in the brain. *J Neurosci* 1994;14:5147-5159.
43. Hardy P, Nuyt AM, Abran D, St-Louis J, Varma DR, Chemtob S. Nitric oxide in retinal and choroidal blood flow autoregulation in newborn pigs: interactions with prostaglandins. *Pediat Res* 1996;39:487-493.
44. Koss MC. Functional role of nitric oxide in regulation of ocular blood flow. *Eur J Pharmacol* 1999;374:161-174.

45. Schmetterer L, Krejcy K, Kastner J, Wolzt M, Gouya G, Findl O, Lexer F, Breiteneder H, Fercher AF, Eichler HG. The effect of systemic nitric oxidesynthase inhibition on ocular fundus pulsations in man. *Exp Eye Res* 1997;64:305-312.
46. Hangai M, Miyamoto K, Hiroi K, Tuijikawa A, Ogura Y, Honda Y, Yoshimura N. Roles of constitutive nitric oxide synthase in postischemic rat retina. *Invest Ophthalmol Vis Sci* 1999;40:450-458.
47. Lam TT, Tso MO. Nitric oxide synthase (NOS) inhibitors ameliorate retinal damage induced by ischemia in rats. *Res Commun Mol Pathol Pharmacol* 1996;92:329-340.
48. Neufeld AH, Hernandez MR, Gonzalez M. Nitric oxide synthase in the human glaucomatous optic nerve head. *Arc. Ophthalmol* 1997;115:497-503.
49. Neufeld AH, Sawada A, Becker B. Inhibition of nitric-oxide synthase 2 by aminoguanidine provides neuroprotection of retinal ganglion cells in a rat model of chronic glaucoma. *Proc Nat Acad Sci U.S.A.* 1996;96:9944-9948.
50. Dimmeler S, Zeiher AM. Nitric oxide and apoptosis: another paradigm for the double-edged role of nitric oxide. *Nitric Oxide* 1997;1:275-281.
51. Vorwerk, CK, Hyman BT, Miller JW, Husain D, Zurakowski D, Huang PL, Fishman MC, Dreyer EB. The role of neuronal and endothelial nitric oxide synthase in retinal excitotoxicity. *Invest Ophthalmol Vis Sci* 1997;38:2038-2044.
52. Siu AW, Reiter RJ, To CH. The efficacy of vitamin E and melatonin as antioxidants against lipid peroxidation in rat retinal homogenates. *J Pineal Res* 1998;24:239-244.
53. Beckman JS, Beckman TW, Chen J, Marshall PA, Freeman BA. Apparent hydroxyl radical production by peroxynitrite: implications for endothelial injury

- from nitric oxide and superoxide. Proc Nat Acad Sci U.S.A. 1990;87:1620-1624.
54. Harman D. Free radical theory of aging. Muta. Re. 1992; 275:257-266.
55. Siu A., Reiter RJ, To CH. Pineal indoleamines and vitamin E reduce nitric oxide-induced lipid peroxidation in rat retinal homogenates. J Pineal Res 1997;27:122-128.
56. Nakayama M, Yasue H, Yoshimura M, Shimasaki Y, Kugiyama K, Ogawa H, Motoyama T, Saito Y, Ogawa Y, Miyamoto Y, Nakao K. T<sup>-786</sup> → C Mutation in the 5'-flanking region of the endothelial nitric oxide synthase gene is associated with coronary spasm. Circulation 1999;99:2864-2870.
57. Farrell AJ, Blake DR, Palmer RMJ, Moncada S. Increased concentrations of nitrite in synovial fluid and serum samples suggest increased nitric oxide synthesis in rheumatic diseases. Ann Rheum Dis 1992;51:1219-1222.
58. Klebanoff S. Reactive nitrogen intermediates and antimicrobial activity: role of nitrite. Free Radic Bio Med 1993;14:351-360.
59. Eiserich JP, Cross CE, Jones AD, Halliwell B, van der Vliet A. Formation of nitrating and chlorinating species by reaction of nitrite with hypochlorous acid. J Biol Chem 1996;271:19199-19208.
60. Eiserich JP, Hristova M, Cross CE, Jines AD, Freeman BA, Halliwell B, van der Vliet A. Formation of nitric oxide-derived inflammatory oxidants by myeloperoxidase in neutrophils. Nature 1998;391:393-397.
61. van der Vliet A, Eiserich JP, Halliwell B, Cross CE. Formation of reactive nitrogen species during peroxidase-catalyzed oxidation of nitrite. J Biol Chem 1997;272:7617-7625.
62. Miyamoto Y, Saito Y, Kajiyama N, Yoshimura M, Shimasaki Y, Nakayama M, Kamitani S, Harada M, Ishikawa M, Kuwahara K, Ogawa E, Hamanaka I,

- Takahashi N, Kaneshige T, Teraoka H, Akamizu T, Azuma N, Yoshimasa Y, Yoshimasa T, Itoh H, Masuda I, Yasue H, Nakao K. Endothelial nitric oxide synthase gene is positively associated with essential hypertension. *Hypertension* 1998;32:3-8.
63. Pecoits-Filho R, Stenvinkel P, Marchlewska A, Heimbürger O, Barant P, Hoff CM. A functional variant of the myeloperoxidase gene is associated with cardiovascular disease in end-stage renal disease patients. *Kidney International* 2003;supplement:S172-176.
64. Kirwan RP, Crean JK, Fenerty CH, Clark AF, O'Brien CJ. Effect of cyclical mechanical stretch and exogenous transforming growth factor-beta1 on matrix metalloproteinase-2 activity in lamina cribrosa cells from the human optic nerve head. *J Glaucoma* 2004;13:327-334.
65. Golubnitschaja O, Wunderlich K, Decker C, Monkemann H, Schild HH, Flammer J. Molecular imaging of perfusion disturbances in glaucoma. *Amino Acids* 2002;23:293-299.
66. Wehrwein E, Thompson SA, Coulibaly SF, Linn DM, Linn CL. Acetylcholine protection of adult pig retinal ganglion cells from glutamate-induced excitotoxicity. *Invest Ophthalmol Vis Sci* 2004;45:1531-1543.
67. Koss MC. Functional role of nitric oxide in regulation of ocular blood flow. *Eur J Pharmacol* 1999;374: 161-174.
68. Romano C, Li Z, Arendt A, Hargrave PA, Wax MB. Epitope mapping of anti-rhodopsin antibodies from patients with normal pressure glaucoma. *Invest Ophthalmol Vis Sci* 1999;40:1275-1280.
69. Tezel G, Hernandez R, Wax MB. Immunostaining of heat shock proteins in the retina and optic nerve head of normal and glaucomatous eyes. *Arch Ophthalmol* 2000;118:511-518.

70. Lipton SA, Rosenberg RA. Mechanisms of disease: Excitatory amino acids as a final common pathway in neurologic disorders. *N Engl J Med* 1994;330:613–622.
71. Lucas DR, Newhouse JP. The toxic effect of sodium l-glutamate on the inner layers of the retina. *Am Med Assoc Arch Ophthalmol* 1957;58:193–201.
72. Olney JW, Ho OL: Brain damage in infant mice following oral intake of glutamate, aspartate or cysteine. *Nature* 1970;227:609–611.
73. Olney JW. Glutamate-induced retinal degeneration in neonatal mice: electron microscopy of the acutely evolving lesion. *J Neuropathol Exp Neurol* 1969;28:455–474.
74. Lipton SA. Molecular mechanisms of trauma-induced neuronal degeneration. *Curr Opin Neurol Neurosurg* 1993;6:588–596.
75. Dreyer EB, Grosskreutz CL. Excitatory mechanisms in retinal ganglion cell death in primary open angle glaucoma (POAG). *Clin Neurosci* 1997;4:270–273.
76. Dreyer EB, Lipton SA: New perspectives on glaucoma. *JAMA* 1999;281:306–308.
77. Dreyer EB, Zhang D, Lipton SA. Transcriptional or translational inhibition blocks low dose NMDA-mediated cell death. *Neuro Report* 1995;6:942–944.
78. Vorwerk CK, Lipton SA, Zurakowski D. Chronic low dose glutamate is toxic to retinal ganglion cells: toxicity blocked by memantine. *Invest Ophthalmol Vis Sci* 1996;37:1618–1624.
79. Brooks DE, Barcia GA, Dreyer EB. Vitreous body glutamate concentration in dogs with glaucoma. *Am J Vet Res* 1997;58:864–867.
80. Dreyer EB, Zurakowski D, Schumer RA. Elevated glutamate in the vitreous body of humans and monkeys with glaucoma. *Arch Ophthalmol* 1996;114:299–305.

81. Zeevalk GD, Nicklas WJ. Evidence that the loss of the voltage-dependent  $Mg^{2+}$  block of the N-methyl-d-aspartate receptor underlies receptor activation during inhibition of neuronal metabolism. *J Neurochem* 1992;59:1211–1220.
82. Bonfoco E, Krainc D, Ankarcrona M, et al. Apoptosis and necrosis: two distinct events induced respectively by mild and intense insults with NMDA or nitric oxide/superoxide in cortical cell cultures. *Proc Natl Acad Sci USA* 1995;92:7162–7166.
83. Budd SL, Tenneti L, Lishnak T, Lipton SA. Mitochondrial and extramitochondrial apoptotic signaling pathways in cerebrocortical neurons. *Proc Natl Acad Sci USA* 2000;97:6161–6166.
84. Dawson VL, Dawson TM, Bartley DA. Mechanisms of nitric oxide-mediated neurotoxicity in primary brain cultures. *J Neurosci* 1993;13:2651–2661.
85. Dawson VL, Dawson TM, London ED. Nitric oxide mediates glutamate neurotoxicity in primary cortical cultures. *Proc Natl Acad Sci USA* 1991;88:6368–6332. Brooks DE, Barcia GA, Dreyer EB. Vitreous body glutamate concentration in dogs with glaucoma. *Am J Vet Res* 1997;58:864–867.
86. Lipton SA, Choi Y-B, Pan Z-H. A redox-based mechanism for the neuroprotective and neurodestructive effects of nitric oxide and related nitroso-compounds. *Nature* 1993;364:626–632.
87. Okamoto S-I, Li Z, Ju C, Schölkze MN. Dominant-interfering forms of MEF2 generated by caspase cleavage contribute to NMDA-induced neuronal apoptosis. *Proc Natl Acad Sci USA* 2002;99:3974–3979.
88. Tenneti L, DEmlia DM, Troy CM, Lipton SA. Role of caspases in N-methyl-d-aspartate-induced apoptosis in cerebrocortical neurons. *J Neurochem* 1998;71:946–959.
89. Tenneti L, Lipton SA. Involvement of activated caspase-3-like proteases in

- N-methyl-d-aspartate-induced apoptosis in cerebrocortical neurons. *J Neurochem* 1000;74:134–142.
90. Kaul M, Garden GA, Lipton SA. Pathways to neuronal injury and apoptosis in HIV-associated dementia. *Nature* 2001;410:988-994.
91. Dreyer EB, Zurakowski D, Schumer RA, et al. Elevated glutamate levels in the vitreous body of humans and monkeys with glaucoma. *Arch Ophthalmol* 1996;114:299–305.
92. Brooks DE, Garcia GA, Dreyer EB, et al. Vitreous body glutamate concentration in dogs with glaucoma. *Am J Vet Res* 1997;58:864–867.
93. Sucher NJ, Wong LA, Lipton SA. Redox modulation of NMDA receptor-mediated Ca<sup>2+</sup> flux in mammalian central neurons. *Neuroreport* 1990;1:29–32.
94. Sucher NJ, Aizenman E, Lipton SA. *N*-methyl-D-aspartate antagonists prevent kainate neurotoxicity in rat retinal ganglion cells in vitro. *J Neurosci* 1991;11:966–971.
95. Hollman PC, Katan MB. Absorption, metabolism and health effects of dietary flavonoids in man. *Biomed Pharmacother* 1997;51:305-310.
96. Hollman PC, Katan MB. Dietary flavonoids: intake, health effects and bioavailability. *Food Chem Toxicol* 1999;37:937-942.
97. Hertog MGL, Hollman PCH. Potential health effects of the dietary flavonol quercetin. *Eur J Clin Nutr* 1996;50:63-71.
98. Hollman PC, van Trijp LM, Buysman MN, et al. Relative bioavailability of the antioxidant flavonoid quercetin from various foods in man. *FEBS Lett* 1997;418:152-156.
99. Hertog MG, Feskens EJ, Hollman PC, Katan MB, Kromhout D. Dietary



- antioxidant flavonoid and risk of coronary heart disease: the Zutphen Elderly Study. *Lancet* 1993;342:1107-1101.
100. Hertog MG, Kromhout D, Aravanis C, Blackburn H, Buzina R, Fidanza F, Giampaoli S, Jansen A, Menotti A, Nedeljkovic S. Flavonoid intake and long-term risk of coronary heart disease and cancer in the seven countries study. *Arch Intern Med* 1995;155:381-386.
101. Middleton EJ Effect of plant flavonoids on immune and inflammatory cell function, *Adv Exp Med Biol* 1998;439:175-182.
102. Wang HK, Xia Y, Yang ZY, Natschke SL, Lee KH. Recent advances in discovery and development of flavonoids and their analogues as antitumor and anti-HIV agents. *Adv Exp Med Biol* 1998;439:191-225.
103. Knekt P, Jarvinen R, Seppanen R, Hellewaara M, Teppo L, Pukkala E, Aromaa A. Dietary flavonoids and the risk of lung cancer and other malignant neoplasms. *Am J Epidemiol* 1997;146:223-230.
104. Pietta PG. Flavonoids as antioxidants. *J Nat Prod* 2000;63:1035-1042.
105. Spencer JPE, Schroeter H, Crossthwaithe AJ, Kuhnle G, Williams RJ, Rice-Evans C. Contrasting influences of glucuronidation and O-methylation of epicatechin on hydrogen peroxide-induced cell death in neurons and fibroblasts. *Free Radic Biol Med* 2001;31:1139–1146.
106. Ishige K, Schubert D, Sagara Y. Flavonoids protect neuronal cells from oxidative stress by three distinct mechanisms. *Free Radical Biol Med* 2001;30:433–446.
107. Hollman PC, Bijman MN, van Gameren Y, Cnossen EP, de Vries JH, katan MB. The sugar moiety is a major determinant of the absorption of dietary flavonoid glycosides in man. *Free Radic Res* 1999;31:569-573.
108. Olthof M, Hollman PCH, Vree TB, fatan MB. Bioavailabilities of

- quercetin-3-glucoside and quercetin-4'-glucoside do not differ in human. *J Nutr* 2000;130:1200-1203.
109. Hsiu SL, Huang TY, Hou YC, Chin DH, Chao PDL. Comparison of metabolic pharmacokinetics of naringin and naringenin in rabbits. *Life Sci* 2002;70:1481-1489.
110. Chang CW, Hsiu SL, Wu PP, Kuo SC, Chao PDL. HPLC assay of naringin and hesperidin in Chinese herbs and serum. *J Food Drug Anal* 1997;5:111-120.
111. Naderi GA, Asgary S, Sarraf-Zadegan N, Oroojy H, Afshin-Nia F. Antioxidant activity of three extracts of *Morus nigra*. *Phytother Res* 2004;18:365-369.
112. Matsubara Y, Yusa T, Sawabe A, Iizuka Y, Takekuma S, Yoshida Y. Structures of new cyclic peptides in young unshiu (*Citrus unshiu* Marcov.), orange (*Citrus sinensis* Osbeck.) and amanatsu (*Citrus natsudaidai*) peelings. *Agric Biol Chem* 1991;55:2923-2929.
113. Chen G, Zhang L, Zhao J, Ye J. Determination of hesperidin and synephrine in *Pericarpium Citri Reticulatae* by capillary electrophoresis with electrochemical detection. *Anal Bioanal Chem* 2002;373:169-173.
114. Wang JF, Guo YX, Niu JZ, Liu J, Wang LQ, Li PH. Effects of *Radix Puerariae* flavones on liver lipid metabolism in ovariectomized rats. *World J Gastroenterol* 2004;10:1967-1970.
115. Alves D, Perez-Fons L, Estepa A, Micol V. Membrane-related effects underlying the biological activity of the anthraquinones emodin and barbaloin. *Biochem Pharmacol* 2004;68:549-561.
116. Mijatovic S, Maksimovic-Ivanic D, Radovic J, Popadic D, Momcilovic M, Harhaji L, Miljkovic D, Trajkovic V. Aloe-emodin prevents cytokine-induced tumor cell death: the inhibition of auto-toxic nitric oxide release as a potential mechanism. *Cell Mol Life Sci* 2004;61:1805-1815.

117. Lu HF, Sue CC, Yu CS, Chen SC, Chen GW, Chung JG. Diallyl disulfide (DADS) induced apoptosis undergo caspase-3 activity in human bladder cancer T24 cells. *Food Chem Toxicol* 2004;42:1543-1552.
118. Lee YM, Wu TH, Chen SF, Chung JG. Effect of 5-methoxypsoralen (5-MOP) on cell apoptosis and cell cycle in human hepatocellular carcinoma cell line. *Toxicol in Vitro* 2003;17:279-287.
119. Chung JG, Yeh KT, Wu SL, Hsu NY, Chen GW, Yeh YW, Ho HC. Novel transmembrane GTPase of non-small cell lung cancer identified by mRNA differential display. *Cancer Res* 2001;61:8873-8879.
120. Park EK, Kwon KB, Park KI, Park BH, Jhee EC. Role of Ca<sup>+2</sup> in diallyl disulfide-induced apoptotic cell death of HCT-15 cells. *Exp Mol Med* 2002;34:250-257.
121. Hehner SP, Heinrich M, Bork PM, Vogt M, Ratter F, Lehmann V, Schulze-Osthoff K, Droge W, Schmitz ML. Sesquiterpene lactones specifically inhibit activation of NF-kappa B by preventing the degradation of I kappa B-alpha and I kappa B-beta. *J Biol Chem* 1998;273:1288-1297.
122. Terry, D.E., Umstot E. and Desiderio D.M. Optimized sample-processing time and peptide recovery for the mass spectrometric analysis of protein digests. *J Am Soc Mass Spectrom* 2004;15:784-794.
123. Hirosawa, M., Hoshida, M., Ishikawa, M., Toya, T. *Comput. Appl. Biosci.* 1993;9:161-167.
124. Kwong JM, Lam TT. N -methyl- D -aspartate (NMDA) induced apoptosis in adult rabbit retinas. *Experimental eye research* 2000;71:437-444.
125. Livak, K.J., Schmittgen, T.D. Analysis of relative gene expression data using real-time quantitative PCR and the 2(-Delta Delta C(T)) Method. *Methods* 2001; 25:402-408.

126. Keirsebilek A, Van Hoorde L, Gao Y, De Bruyne G, Bruyneel E, Vermassen P, Mareel M, van Roy F. Mechanisms of downregulation of transfected E-cadherin cDNA during formation of invasive tumors in syngeneic mice. *Invasion and Metasis* 1998;18:44-56.
127. Fu L, Benchimol S. Participation of the human p53 3'UTR in translational repression and activation following  $\gamma$ -irradiation 1997;16:4117-4125.
128. Lee Wy, Loflin P, Clancey CJ, Peng H, Lever JE. Cyclic nucleotide regulation of Na<sup>+</sup>/glucose cotransporter (SGLT1) mRNA stability. Interaction of a nucleocytoplasmic protein with a regulatory domain in the 3'-untranslated region critical for stabilization. 2000;275:33998-34008.
129. Nathanson JA. Nitric oxide and nitrovasodilators in the eye: Implication for ocular physiology and glaucoma. *J Glaucoma* 1993;2:206-210.
130. Schuman JS, Erickson K, Nathanson JA. Nitrovasodilator effects on intraocular pressure and outflow facility in monkeys. *Exp Eye Res* 1994;58:99-105.
131. Nathanson JA, McKee M. Alterations of ocular nitric oxide synthase in human glaucoma. *Invest Ophthalmol Vis Sci* 1995;36:1774-1784.
132. Haefliger IO, Dettmann E, Liu R, Meyer P, Prunte C, Messerli J, Flammer J. Potential role of nitric oxide and endothelin in the pathogenesis of glaucoma. *Surv Ophthalmol Supplement* 1999;1:S51-S58.
133. Chang CJ, Chiang CH, Chow JC, Lu DW. Aqueous humor nitric oxide levels differ in patients with different types of glaucoma. *J Ocul Pharmacol Ther* 2000;5:399-406.
134. Galassi F, Sodi A, Ucci F, Renieri G, Pieri G, Masini E. Ocular dynamics and nitric oxide in normal pressure glaucoma. *Acta Ophthalmol Scand Supplement* 2000;78:37-38.

135. Moncada S, Palmer RM, Higgs EA. Nitric oxide: physiology, pathophysiology, and pharmacology. *Pharmacol Rev* 1991;43:209-242.
136. Anderson RE, Maude MB. Phospholipids of bovine outer segments. *Biochemistry* 1970;9:3264-3268
137. Murphy MP. Nitric oxide and cell death. *Biochim Biophys Acta* 1999;1411:401-414.
138. Hangai M., Yoshimura N, Hiroi K, Mandai M, Honda Y. Inducible nitric oxide synthase in retinal ischemia-reperfusion injury. *Exp Eye Res* 1996;63:501-519.
139. Oku H, Yamaguchi H, Sugiyama T, Kojima S, Ota M, Azuma I. Retinal toxicity of nitric oxide released by administration of a nitric oxide donor in the albino rabbit. *Invest Ophthalmol Vis Sci* 1997;38:2540-2544.
140. Beckman JS, Chen J, Ischiropoulos H, Crow JP. Oxidative chemistry of peroxynitrite. *Methods Enzymol* 1994;233:229-240.
141. Koss MC. Functional role of nitric oxide in regulation of ocular blood flow. *Eur J Pharmacol* 1999;374:161-174.
142. Nathanson JA. Nitrovasodilators as a new class of ocular hypotensive agents. *J Pharmacol E Ther* 1992;260:956-965.
143. Kubota R, Noda S, Wang Y, Minoshima S, Asakawa S, Kudoh J, Mashima Y, Oguchi Y, Shimizu N. A novel myosin-like protein (myocilin) expressed in the connecting cilium of photoreceptor molecular cloning, tissue expression, and chromosomal mapping. *Genomica* 1997;41:360-369.
144. Takahashi H, Noda S, Imamura Y, Nagasawa A, Kubota R, Mashima Y, Kudoh J, Oguchi Y, Shimizu N. Mouse myocilin (Myoc) gene expression in ocular tissues. *Biochem Biophys Res Commun.* 1998;248:104-109.
145. Mijatovic S, Maksimovic-Ivanic D, Radovic J, Popadic D, Momcilovic M,

- Harhaji L, Miljkovic D, Trajkovic V. Aloe-emodin prevents cytokine-induced tumor cell death: the inhibition of auto-toxic nitric oxide release as a potential mechanism. *Cell Mol Life Sci.* 2004;61:1805-1815.
146. Liang JW, Hsiu SL, Wu PP, Chao PDL. Emodin pharmacokinetics in rabbits. *Planta Medica* 1995;61:406-408.
147. Hsiu SL, Huang TY, Hou YC, Chin DH, Chao PDL. Comparison of metabolic pharmacokinetics of naringin and naringenin in rabbits. *Life Science* 2002;70:1481-1489.
148. Fang SH, Hou YC, Chang WC, Hsiu SL, Chao PDL, Chiang BL. Morin sulfates/glucuronides exert anti-inflammatory activity on activated macrophages and decreased the incidence of septic shock. *Life Science* 2003;74:743-756.
149. Yang JH, Hsia TC, Kuo HM, Chao PD, Chou CC, Wei YH, Chung JG. Inhibition of lung cancer cell growth by quercetin glucuronides via G2/M arrest and induction of apoptosis. *Drug Metab Dispos.* 2006;34:296-304.
150. Olney JW, Ho OL. Brain damage in infant mice following oral intake of glutamate, aspartate or cysteine. *Nature* 1970;227:609-611.
151. Lipton SA, Rosenberg RA. Mechanisms of disease: Excitatory amino acids as a final common pathway in neurologic disorders. *N Engl J Med* 1994;330:613-622.
152. Lesnikov VA, Abbasi N, Lesnikova MP, Lazaro CA, Campbell JS, Fausto N, Deeg HJ. Protection of human and murine hepatocytes against Fas-induced death by transferrin and iron. *Apoptosis* 2006;11:79-87.
153. Calabrese V. Highlight Commentary on "Redox proteomics analysis of oxidatively modified proteins in G93A-SOD1 transgenic mice-A model of familial amyotrophic lateral sclerosis". *Free Radic Biol Med* 2007;43:160-162.
154. Witt AE, Hines LM, Collins NL, Hu Y, Gunawardane RN, Moreira D, Raphael

- J, Jepson D, Koundinya M, Rolfs A, Taron B, Isakoff SJ, Brugge JS, LaBaer J. Functional proteomics approach to investigate the biological activities of cDNAs implicated in breast cancer. *J Proteome Res* 2006;5:599-610.
155. Lovegrove C. Galectin-1: a novel hypoxia-induced protein linked with tumor immune privilege. *Nat Clin Pract Oncol* 2006;3:6.
156. Tomlinson VA, Newbery HJ, Wray NR, Jackson J, Larionov A, Miller WR, Dixon JM, Abbott CM. Translation elongation factor eEF1A2 is a potential oncoprotein that is overexpressed in two-thirds of breast tumours. *BMC Cancer* 2005;5:113.
157. Rylander MN, Feng Y, Bass J, Diller KR. Thermally induced injury and heat-shock protein expression in cells and tissues. *Ann N Y Acad Sci* 2006;1066:222-242.
158. Zhang HW, Wang FS, Shao W, Zheng XL, Qi JZ, Cao JC, Zhang TM. *Biochemistry (Mosc)*. Characterization and stability investigation of Cu,Zn-superoxide dismutase covalently modified by low molecular weight heparin. 2006;71:96-100.
159. Okada SF, O'Neal WK, Huang P, Nicholas RA, Ostrowski LE, Craigen WJ, Lazarowski ER, Boucher RC. Voltage-dependent anion channel-1 (VDAC-1) contributes to ATP release and cell volume regulation in murine cells. *J Gen Physiol*. 2004;124:513-526.
160. Myung JK, Gulesserian T, Fountoulakis M, Lubec G. Deranged hypothetical proteins Rik protein, Nit protein 2 and mitochondrial inner membrane protein, Mitofilin, in fetal Down syndrome brain *Cell Mol Biol (Noisy-le-grand)* 2003;49:739-746.
161. Ciaffi M, Paolacci AR, D'Aloisio E, Tanzarella OA, Porceddu E. Cloning and characterization of wheat PDI (protein disulfide isomerase) homoeologous

genes and promoter sequences. *Gene* 2006;366:209-218.

162. Ben Simon GJ, Bakalash S, Aloni E, Rosner M. A Rat Model for Acute Rise in intraocular pressure: immune modulation as a therapeutic strategy. *Am J Ophthalmol* 2006;141:1105-1111.